THESIS FOR THE DEGREE OF LICENTIATE OF ENGINEERING

Renormalization-Group Invariant Formulation of Chiral Effective Field Theory Applied to the Nucleon-Nucleon System

Oliver Thim

Department of Physics
Chalmers University of Technology
Gothenburg, Sweden 2023

Renormalization-Group Invariant Formulation of Chiral Effective Field Theory Applied to the Nucleon-Nucleon System

Oliver Thim

This thesis has been prepared using LaTeX.

Department of Physics
Chalmers University of Technology
SE-412 96 Gothenburg
Sweden
Telephone +46 (0)31-772 1000

Cover: Illustration of a singular potential that causes the reduced radial wave function to oscillate infinitely fast which prohibits a well-defined solution to the Schrödinger equation.

Printed by Chalmers digitaltryck
Gothenburg, Sweden 2023

Renormalization-Group Invariant Formulation of Chiral Effective Field Theory Applied to the Nucleon-Nucleon System

Oliver Thim
Department of Physics
Chalmers University of Technology

Abstract

Chiral effective field theory (χEFT) promises a systematically improvable description of the strong interaction between nucleons consistent with the symmetries of quantum chromodynamics (QCD). A sound power counting (PC) scheme is vital to organize the order-by-order contributions of interaction diagrams to nuclear observables in compliance with renormalization-group (RG) invariance. Numerical values of the low-energy constants (LECs), governing the strengths of pion-nucleon and nucleon-contact diagrams, must be inferred from data and vary with the high-momentum cutoff to remove any dependence on the arbitrary regularization procedure. To date, most χEFT predictions of nuclear systems rely on a PC introduced in the 1990s that does not comply with RG-invariance. One can argue that the lacking RG-invariance makes the connection with QCD muddled and that predictive power is lost. I have developed Bayesian methods for inferring the probability distributions for the numerical values of the LECs at leading order in a recent and RG-invariant PC by Long and Yang. I find that conditioning the inference on neutron-proton (np) scattering observables, rather than scattering phase shifts as is typically done, significantly impacts the results. Furthermore, I use distorted-wave perturbation theory to compute predictions for low-energy np scattering observables up to the fourth chiral order in this PC using point estimates for the LECs. I find a clear order-by-order improvement in the theoretical description of experimental scattering data. This work is an important step towards enabling a Bayesian analysis of low-energy nuclear observables with the aim of assessing whether χEFT, formulated using an RG-invariant PC, accurately predicts the physics of atomic nuclei.

Publications

This thesis is based on the work contained in the following papers.

I "Bayesian analysis of chiral effective field theory at leading order in a modified Weinberg power counting approach"
O. Thim, E. May, A. Ekström, and C. Forssén
Preprint: arXiv:2302.12624 [nucl-th]
Phys. Rev. C **108**, 054002 (2023)

II "Perturbative computations of nucleon-nucleon scattering observables using χEFT up to N3LO"
O. Thim, A. Ekström, and C. Forssén
(in preparation)

Statement of contributions

My contributions to the included papers were:

I I wrote the code to compute *np* scattering observables and the limit-cycle-like behavior. I also performed the Bayesian inference using MCMC and wrote the first draft of the manuscript which I refined together with my co-authors.

II I contributed to formulating the research idea, I did the necessary derivations for the distorted-wave perturbation series, and implemented and benchmarked the code. I produced the results and drafted the manuscript with my co-authors.

Acknowledgements

First, I would like to extend my sincere gratitude to my supervisors Prof. Andreas Ekström and Prof. Christian Forssén for all the guidance, help, and time they devoted to me during these projects. Additionally, I am grateful to my former and current colleagues in the Theoretical Subatomic Physics group, in particular, Dr. Chieh-Jen Yang, Dr. Sean Miller, Dr. Isak Svensson, Dr. Weiguang Jiang, Dr. Alexandra Roussou, Dr. Håkan T. Johansson, Eleanor May, Dr. Simone Li Muli and Eric Nilsson for guidance and many helpful discussions. I would also like to thank Prof. Bingwei Long and Rui Peng for helpful discussions regarding their work on this subject.

List of acronyms

	Symbols
NN	nucleon-nucleon
χEFT	chiral effective field theory
χPT	chiral perturbation theory
np	neutron-proton
	C
c.m.	center of mass
	D
DWB	distorted-wave Born
	E
EFT	effective field theory
	L
LECs	low-energy constants
LO	leading order
LS	Lippmann-Schwinger
	M
MCMC	Markov chain Monte Carlo
MWPC	modified Weinberg power counting
	N
NDA	naive dimensional analysis
	O
OPE	one-pion-exchange
	P
PC	power counting
pdf	probability density function
ppd	posterior predictive distribution
	Q
QCD	quantum chromodynamics
	R
RG	renormalization group
	W
WPC	Weinberg power counting

Contents

Chapter 1

Introduction

Nuclear physics research strives to describe the inner workings of atomic nuclei and their interactions with other nuclei, matter, and fields. A good understanding of nuclei and their properties plays an important role in the basic as well as applied sciences, e.g., astrophysics, particle physics, and medical physics. This thesis work focuses on the fundamental theoretical description of the strong nuclear interaction, which is responsible for the binding of constituent protons and neutrons in finite nuclei and nuclear matter.

A quantum system of neutrons and protons, collectively referred to as nucleons, is believed to be governed by the time-independent many-body Schrödinger equation

$$H\left|\Psi\right\rangle = E\left|\Psi\right\rangle, \tag{1.1}$$

where $|\Psi\rangle$ denotes a quantum state with energy E, and $H = T + V$ is the Hamiltonian operator consisting of the kinetic energy operator (T) and potential energy operator (V). To obtain $|\Psi\rangle$, one needs two things; a model for V, describing the nuclear interaction, and a method for solving Eq. (1.1). This thesis will mainly focus on the former. For this purpose, Eq. (1.1) will mainly be solved for neutron-proton (np) scattering states ($E > 0$), where the Schrödinger equation can be cast into an equivalent form, called the Lippmann-Schwinger (LS) equation.

Before delving into the details, we will first take a step back and look at how the nuclear interaction has been modeled historically, and what ideas have led up to the present descriptions. Modeling of the atomic nucleus started with its discovery by Rutherford in 1911 [1]. Following Chadwick's discovery of the neutron in 1932 [2], it was suggested that both the proton and the neutron were fundamental constituents of nuclei. The coexistence of neutrons and electrically charged protons in the nucleus prompted the compelling assumption that an attractive force must act between them — the *nuclear force*.

From known binding energies of a variety of nuclei, Wigner [3] inferred that

the nuclear force must be of short range, and relatively strong within that range, which gave the nuclear force its other name: the *strong force*. In 1935, Yukawa [4] proposed that a new elementary particle could be responsible for the strong interaction. This particle was suggested to have a mass somewhere in between that of the electron and the proton. Since 1947 we have known this proposed particle as the pion (π), which indeed plays an important role in modeling the nuclear force.

It was soon understood that the nuclear force carried a complicated structure compared to the other known forces at the time. Building on the ideas of Yukawa, meson-exchange models were created and rather successfully applied to model the nuclear force. In these models, the nuclear force is characterized by the exchange of pions, as well as heavier mesons with varying spin and parity properties, thus imparting unique force characteristics. Following the progress in nucleon-nucleon (NN) scattering experiments and the development of effective range theory [5] in the 1940's, more could be learned about the structure of the nuclear force. Despite the success of the meson-exchange models, there was still a lack of solid theoretical justification for the zoo of different mesons; for a more complete historical review see, e.g., Ref. [6].

The theoretical understanding of the origin of the nuclear force brightened in the 60's and 70's with the formation of quantum chromodynamics (QCD) [7], in which both nucleons and mesons are predicted and described as composite particles consisting of quarks. Following the discovery of QCD, the task of understanding how the strong force among the composite particles emerges from the strong interaction between quarks started. This turned out to be challenging since QCD is highly non-perturbative in the low-energy regime where nuclear physics resides.

A breakthrough came when Weinberg [8] applied the ideas of effective field theory (EFT) to low-energy QCD with the aim of modeling the nuclear force. Even though the underlying theory, QCD, consists of quarks and gluons, the effective theory is formulated in terms of the effective degrees of freedom — in this case nucleons and pions. As dictated by the so-called *folk theorem* [8], the dynamics of the effective degrees of freedom (nucleons and pions) is described by the most general effective Lagrangian consistent with the underlying symmetries of QCD. Besides the spacetime symmetries, the approximate chiral symmetry of low-energy QCD plays an important role in constraining the pion-nucleon interaction, since the pion can be described as a pseudo Nambu-Goldstone boson of this spontaneously broken chiral symmetry [9].

The effective Lagrangian contains an infinite number of pion-pion, pion-nucleon, and nucleon-contact interaction terms [10]. To truncate the Lagrangian in a meaningful way, and only consider the most important terms, some principle is needed to assess their relative importance. This kind of organizational principle is known as power counting (PC). Since the EFT is a low-energy effective description of QCD, it is expected to be accurate below a certain momentum

scale, called the breakdown scale (Λ_b), whose exact value is unknown a priori. The breakdown scale can however be estimated to be of the order where neglected explicit degrees of freedom become important, such as heavier mesons, e.g. $\rho(770)$.

Using a PC scheme, a chiral order (ν) can be assigned to each Feynman diagram emerging from the effective Lagrangian. The chiral order describes the scaling of the given diagram as $(Q/\Lambda_b)^\nu$, where Q denotes the relevant low-energy scale, which in the case of NN scattering could be the center of mass (c.m.) external momenta, and the pion mass. The orders $\nu = 0, 1, 2, ...$ will also be denoted as leading order (LO), next-to-leading order (NLO), next-to-next-to-leading order ($\mathrm{N^2LO}$) and so on. Crucial to the success of the EFT framework is that the relevant low-energy scales are much smaller than the breakdown scale Λ_b, which means that only relatively low-energy phenomena are expected to be accurately captured by the EFT.

Following Weinberg's EFT idea, Gasser et al. [11, 12] worked out pion-pion ($\pi\pi$) and pion-nucleon (πN) scattering in perturbation theory to one loop. This EFT, including at most one nucleon, is referred to as chiral perturbation theory (χPT). In the past decades, χPT has seen great success, see, e.g., Ref. [13].

In the multi-nucleon sector, where the EFT is referred to as chiral effective field theory (χEFT), the theoretical description turns out to be more challenging since a non-perturbative treatment is required due to the existence of nuclear bound states. In a series of papers [14–16], Weinberg proposed calculating nuclear amplitudes by first deriving NN potentials perturbatively from the chiral Lagrangian using χPT followed by inserting the potentials in the Schrödinger or LS equation. This canonical approach is referred to as Weinberg power counting (WPC), and will be discussed in Chapter 2.

It is interesting to conclude that more than half a century after the proposal by Yukawa, the pion is reborn as an effective degree of freedom emerging as a pseudo Nambu-Goldstone boson of the spontaneously broken chiral symmetry of low-energy QCD. Although simple, the pion-exchange process is a central part of the nuclear force and will be discussed in much detail in this thesis.

Using WPC, Ordonez et al. [17–19] derived NN potentials up to order $\nu = 3$ in time-ordered perturbation theory in the early 90's. With those works, the era of constructing quantitative nuclear forces from χEFT began. Kaiser et al. [20–24] applied covariant perturbation theory and dimensional regularization to study perturbative NN amplitudes up to $\nu = 3$, as well as working out loop contributions of high orders. Epelbaum et al. [25–27] constructed potentials with the method of unitary transformations up to $\nu = 4$, which eliminated the scattering energy dependence of the potentials. Furthermore, Epelbaum et al. [28] also computed three-nucleon forces, which arise naturally. The natural description of many-nucleon forces is one of the great strengths of χEFT. In 2003, Entem et al. constructed potentials up to $\nu = 4$ [29] and demonstrated that one can achieve sufficient precision for describing NN scattering and nuclear

structure at this order.

Although χEFT provides strong constraints on the possible interaction terms through symmetries, the strength of the interaction terms is parametrized by so-called low-energy constants (LECs) whose values are a priori undetermined. Calibration of the LECs can, for example, be performed by minimizing some χ^2 measure using experimental NN scattering phase shifts or observables [29, 30]. A significant advantage of working with an EFT model is that the theoretical (or model) error emerges naturally in the description and can be quantified via the $(Q/\Lambda_b)^\nu$ expansion. An early attempt to utilize this was made by Carlsson et al. [31] where an estimated EFT model error, as well as bound state ($E < 0$) observables, were used in the calibration of LECs.

In later years, Bayesian inference methods have been employed for the calibration of WPC interactions with the benefit of systematically quantifying both the experimental and EFT model errors [32–40]. The Bayesian framework is ideal for properly including prior assumptions as well as for offering a probabilistic interpretation of uncertainties in the LECs and predicted observables. Assessing both experimental and model errors and their impact on the resulting theoretical predictions is a crucial element for enabling precision studies of nuclear observables.

To date, WPC is the dominating approach to construct NN forces, and it has been used to construct χEFT NN interactions up to $\nu = 5$ [41, 42]. Combining the chiral forces with methods to solve the Schrödinger equation, such as the no-core shell model [43] or coupled cluster theory [44], has enabled the study of nuclei from an *ab initio* perspective during the last decades [45–47]. In recent years, *ab initio* computations have advanced to encompass increasingly heavier systems, including the nuclei ^{48}Ca, ^{132}Sn, and ^{208}Pb [48–50]. In particular, the neutron skin thickness of heavy nuclei is linked to the structure and size of neutron stars via the neutron-matter equation of state [51–53]. This means that *ab initio* predictions can connect multimessenger astrophysical information with the EFT description of the nuclear force [50, 54], which in turn connect to QCD and the Standard Model. Beyond the study of nuclear properties, precision *ab initio* studies of nuclear physics can also be applied to study fundamental symmetries and physics beyond the Standard Model. One example is the study of the unitarity of the Cabibbo-Kobayashi-Maskawa quark mixing matrix, which requires electroweak radiative corrections from nuclear theory [55, 56]. Another is the study of neutrinoless double beta decay ($0\nu\beta\beta$). This is a hypothetical radioactive process that, if observed, would be a first signal of lepton number violation and would prove that the neutrino is a Majorana fermion and its own antiparticle [57, 58].

A cornerstone in theoretical *ab initio* studies is the modeling of the nuclear interaction, and doing so in a statistically sound manner by the inclusion of quantified uncertainties. It is here my work enters. To date, the dominating PC used to construct nuclear interactions and study the above questions is

WPC. Although quite successful, theoretical investigations of WPC — already several decades ago — indicated that WPC did not provide amplitudes that are renormalized order by order [59], which was later confirmed by numerical studies [60, 61]. What this means is that the physical predictions acquire a dependence on the specific regularization procedure used to separate short- and long-range physics in the process of renormalization. Renormalization group (RG) invariance is the requirement that physical predictions at each order in the EFT are independent of the arbitrary regularization procedure. It can be argued that the lack of RG invariance in WPC leads to the connection with QCD becoming muddled, and predictive power being reduced.

Using lessons from a simpler nuclear EFT, including only nucleons, Kaplan et al. [62, 63] proposed a PC for χEFT where pions are added in perturbation theory, which would remove the renormalization problems in χEFT. Unfortunately, this scheme did not improve the range of convergence in momenta beyond what was achievable in an EFT completely without pions [64].

The origin of the renormalization problems in χEFT can be traced to the fact that the emerging potentials are singular [65, 66]. Singular potentials can still produce RG-invariant amplitudes provided that divergence absorbing counterterms are included [60]. But, the addition of counterterms in the infinitely many partial waves where the potential is singular would introduce an infinite number of LECs, and ruin the predictive power. Fortunately, since the centrifugal barrier weakens the singular potential for high angular momentum, new counterterms are only needed in a few partial waves, namely those with angular momentum quantum number $\ell < \ell_c$, for $\ell_c \approx 2$ [67, 68]. Potentials beyond LO are in general increasingly singular. However, Long and van Kolck [69] have shown that no additional counterterms need to be added beyond the ones already present, as long as sub-leading potential corrections are treated in perturbation theory.

Based on these findings, several modifications of WPC have been proposed and studied [61, 68, 70–78]. Good overviews are contained in Refs. [79, 80]. A proposal dating back to 2005 [60] is to modify the PC by Kaplan et al. and treat pions perturbatively *only* in partial waves with $\ell \geq \ell_c$. The argument is that the interaction is sufficiently strong in the first few partial waves to require a non-perturbative treatment.

The approach of including pions partly perturbatively was further developed by Long and Yang in Refs. [75–77]. They analyzed partial wave amplitudes in detail to determine at which order certain counterterms with associated LECs should appear to retain RG invariance at each order. In their study, they computed *np* scattering phase shifts up to N^{2}LO, and N^{3}LO in selected channels, finding a satisfactory description of empirical phase shifts [81]. In the light of this new PC proposal, the perturbative investigations of NN scattering initialized in Ref. [68] was further explored in Refs. [67, 82] to include higher-order NN potentials from χEFT.

The PC proposed by Long and Yang is in this thesis referred to as modified Weinberg power counting (MWPC) and will be outlined in Section 2.2. This PC has to date only been used to study a few selected nuclear observables. In Ref. [83], nuclear ground state energies for ^{3}H, ^{3,4}He, ^{6}Li and ^{16}O were studied up to NLO. The resulting binding rendered ^{16}O prone to decay to four α-particles, and ^{6}Li to an α-particle plus a deuteron. The apparent failure can be due to many factors, including a lack of many-nucleon forces and insufficient pion exchanges at LO. Another possible culprit proposed in Ref. [83] is that fine-tuning in the nuclear interaction requires more careful calibration of the LECs. Yang et al. [83] renormalized the LECs by demanding the exact reproduction of selected phase shifts at single scattering energies, which might induce overfitting in the interactions sufficient to produce unphysical results for the studied observables.

The possibility of realistically describing nuclear properties in a PC other than WPC is to date an open problem. This thesis aims to take the first steps to construct interactions with quantified uncertainties using the MWPC developed by Long and Yang. Constructing nuclear interactions with quantified LEC-uncertainties using a PC that complies with RG-invariance is not yet explored and, if done successfully, would provide an entirely new avenue of analyzing properties of finite nuclei and nuclear matter.

The key questions regarding MWPC that will be addressed in this thesis can be summarized as follows:

1. How to infer/calibrate the unknown LECs from data?
2. How to build an accurate model for the EFT truncation error, and how to test it?
3. How well can *np* scattering observables be described?
4. How can the order-by-order convergence be used to learn about the perturbativeness of the χEFT expansion?

Specifically, this thesis will address questions (1) and (2) in Paper I, and (3) and (4) in Paper II. Another important question is how to efficiently compute bound-state observables to sufficiently high orders in perturbation theory. This question and further developments are left for future work. The thesis is organized as follows. Chapter 2 contains a more detailed introduction to χEFT, WPC and MWPC to motivate and understand the potentials and calculations performed in this thesis. Chapter 3 discusses how to compute NN scattering observables in MWPC and presents some key results from the appended Papers I and II. In Chapter 4, the findings and conclusions of this thesis are summarized and future directions of studies are discussed.

Chapter 2

Power Counting in Chiral Effective Field Theory

To describe a nuclear system using the Schrödinger equation (1.1), an interaction potential modeling the strong force is the crucial input. In this chapter, we will discuss how to construct NN potentials in χEFT using appropriate PC schemes. The goal is to motivate the use of the specific MWPC scheme proposed in Refs. [69, 75–77, 79], in which the predicted amplitudes are RG-invariant. Natural units in which $\hbar = c = 1$ will be used in this chapter and throughout the thesis.

2.1 Chiral Effective Field Theory

Quantum chromodynamics (QCD) is to date the most fundamental theory describing the strong interaction in the Standard Model of particle physics. One remarkable property of QCD is that the strong interaction weakens at high energy scales which enables the use of perturbation theory. This is known as asymptotic freedom [84]. On the contrary, the interaction becomes stronger and highly non-perturbative in the low-energy regime of QCD ($\sim$ MeV) relevant to nuclear physics. One way to tackle the non-perturbative problem at low energies is Lattice QCD, which is a numerical approach to solve the full equations of QCD on an Euclidean space-time lattice [85]. While some success is seen, see e.g. Refs. [86, 87], the vast numerical complexity of this method makes large simulations exceedingly challenging and insofar does not present an operational approach to analyze atomic nuclei. Another approach to handle the non-perturbativeness is provided by χEFT, which utilizes an effective (approximate) description of low-energy QCD in terms of more appropriate/effective degrees of freedom trading the quarks and gluons for interacting nucleons and pions. The power of this approximate approach is that it is consistent with

the symmetries of low-energy QCD, systematically improvable and, most importantly, it enables numerical studies of atomic nuclei [50].

An analogy

The EFT paradigm rests on the physical principle that fine details of high-energy physics should not impact low-energy observables. This principle is as old as physics itself since it implicitly has been used throughout history to model physics phenomena without knowing the details of underlying processes at higher-energy scales. The goal of an EFT is therefore to capture the most general dynamics among low-energy degrees of freedom that are consistent with the assumed symmetries of the underlying interaction.

As an example, Fermi's theory of weak interactions [88] can be seen as an EFT of the Standard Model below the mass of the W ($m_W \approx 80$ GeV) and Z ($m_Z \approx 91$ GeV) bosons. The Standard Model amplitude describing β-decay involves an exchange of a W-boson. In β-decay, typical momentum transfers are limited to a few tens of MeV, and hence much less than m_W [89]. This small momentum transfer means that the exchanged W-boson must be highly virtual and thus short-lived. A short lifetime will make the interaction local within a first approximation with corrections of order $\mathcal{O}(q^2/m_W^2)$ where q is the momentum transfer. One advantage of viewing this theory as an EFT is that the impact of corrections from the Standard Model can be systematically computed; another is that the theoretical error, compared to the Standard Model amplitude, can be estimated since we know that the dominant neglected terms should scale as $\mathcal{O}(q^2/m_W^2)$.

The power of χEFT

Chiral symmetry is an important feature of low-energy QCD that can be used to constrain pion-pion and pion-nucleon interactions. This symmetry is not exact, but in fact broken both spontaneously and explicitly. Spontaneous symmetry breaking is known to give rise to massless Nambu-Goldstone bosons. The three pions (π^+, π^-, π^0) can be identified as the pseudo Nambu-Goldstone bosons of the spontaneously broken chiral symmetry. They are not exactly massless as a result of the accompanying explicit symmetry breaking due to the non-zero quark masses. Formulating an effective theory of interacting nucleons and pions as the only degrees of freedom neglects, for example, known heavier mesons such as the ρ meson ($m_\rho \sim 770$ MeV) and nucleon excitations such as the $\Delta(1232)$. As a result, χEFT is only expected to be accurate for momenta where the effects of neglected degrees of freedom can be represented as point-like. This is the fundamental reason for the existence of a breakdown scale, Λ_b, beyond which the predictive power of the χEFT vanishes.

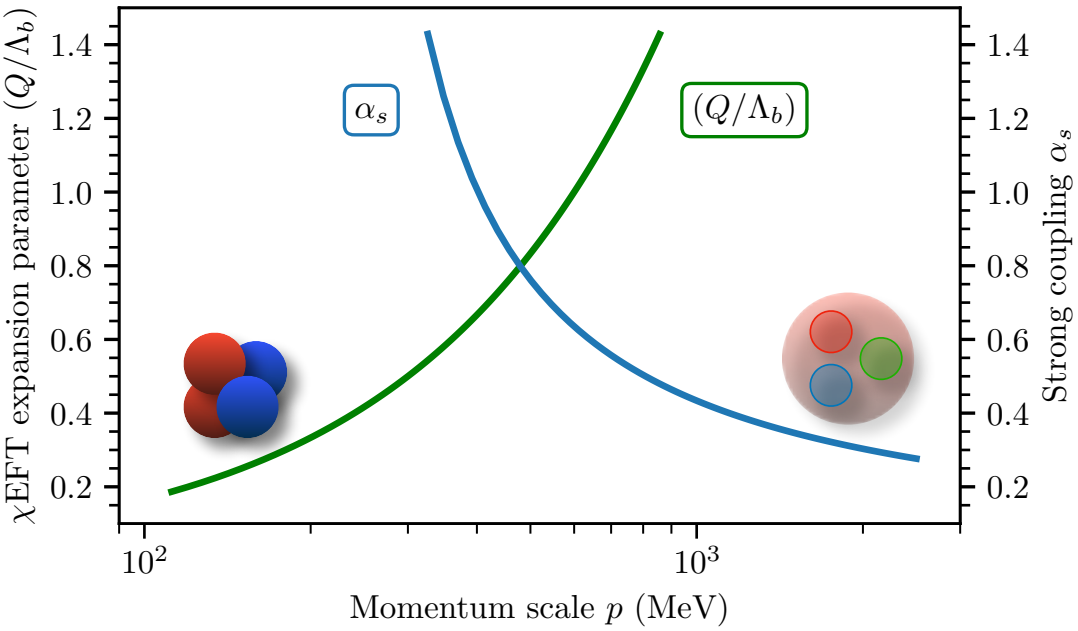

Figure 2.1: Illustration of momentum regimes where QCD and χEFT are perturbative. The blue line shows the approximate running of the strong coupling, α_s, revealing the asymptotic freedom [90]. The χEFT expansion parameter, (Q/Λ_b), shown in green is, on the contrary, small in the low-energy regime relevant to nuclear physics. Here, $\Lambda_b = 600$ in accordance with a recent analysis [35].

Shifting to effective degrees of freedom and utilizing the approximate chiral symmetry in constructing an effective pion-nucleon Lagrangian, low-energy processes involving nucleons and pions can be described in a systematically improvable framework. Such an approach is expected to be accurate at low energies where the low-energy scales $Q \sim p$, m_π are much smaller than Λ_b. Here, p denotes the modulus of the external momentum in the c.m. frame and $m_\pi \approx 138$ MeV is the average pion mass. This is in complete analogy to the example of Fermi's theory.

The power of describing the low-energy regime of QCD in terms of χEFT is illustrated in Fig. 2.1. The strong coupling constant, α_s, governs where QCD can be treated perturbatively, namely when $\alpha_s \ll 1$, which is fulfilled in the high energy regime $p \gtrsim 1$ GeV. This regime is relevant in, for example, high-energy accelerator experiments probing the inner quark-structure of hadrons [90]. On the contrary, χEFT is expanded in powers of $(Q/\Lambda_b)^\nu$, where ν denote the chiral order, and a systematic perturbative treatment is possible in the low-energy ($\sim$ MeV) regime relevant to nuclear physics. The major advantages of using χEFT to describe nuclear forces are:

1. χEFT provides a framework for deriving a low-energy theory that is *rooted in the underlying theory* of QCD through symmetries.

2. χEFT provides a *systematically* improvable description of low-energy observables where the *model error* can be quantified.

3. Many-nucleon interactions and currents, important for describing heavier nuclei and decays, can consistently be derived within χEFT.

In this work, we will only study two-nucleon processes while many-nucleon forces and currents will not be considered. Next, we will delve into how NN potentials are constructed in χEFT by using PC to order contributions. In the next section, we will start to describe WPC.

Weinberg PC and infrared enhancement

To construct an EFT consistent with the underlying theory one has to write down the most general Lagrangian for the considered degrees of freedom respecting the relevant symmetries. Using this principle, the infinite set of Lagrangian terms for χEFT can be derived using the non-linear realization of the spontaneously broken chiral symmetry of low-energy QCD along with relevant space-time symmetries [8]. The effective Lagrangian in the two-nucleon sector can be divided into pion-pion ($\pi\pi$), pion-nucleon (πN), and nucleon-nucleon (NN) parts as

$$\mathcal{L}_{\text{eff}} = \mathcal{L}_{\pi\pi} + \mathcal{L}_{\pi N} + \mathcal{L}_{NN}. \tag{2.1}$$

Each of these terms can be expanded in the power of low-energy scales (Q^ν) appearing [91]

$$\mathcal{L}_{\pi\pi} = \mathcal{L}^{(2)}_{\pi\pi} + \mathcal{L}^{(4)}_{\pi\pi} + \dots \tag{2.2}$$

$$\mathcal{L}_{\pi N} = \mathcal{L}^{(1)}_{\pi N} + \mathcal{L}^{(2)}_{\pi N} + \mathcal{L}^{(3)}_{\pi N} + \dots \tag{2.3}$$

$$\mathcal{L}_{NN} = \mathcal{L}^{(0)}_{NN} + \mathcal{L}^{(2)}_{NN} + \mathcal{L}^{(4)}_{NN} + \dots, \tag{2.4}$$

where the upper index denotes ν. The fact that it is possible to do this expansion gives an effective theory that is predictive for low energies ($Q/\Lambda_b < 1$) since only a finite number of terms will contribute up to a given order ν. To describe non-relativistic systems, it is sufficient to have a non-relativistic expansion of the effective Lagrangian which simplifies the calculations [91]. A common way to compute the non-relativistic expansion is to apply the so-called heavy-baryon formalism, in which nucleons are treated as heavy static sources [92, 93].

Quantum mechanical interaction potentials can be constructed by considering two-nucleon scattering in the c.m. frame described by $\mathcal{L}_{\text{eff}}$. The kinematics of two-nucleon scattering is illustrated in Fig. 2.2 in the laboratory and c.m.

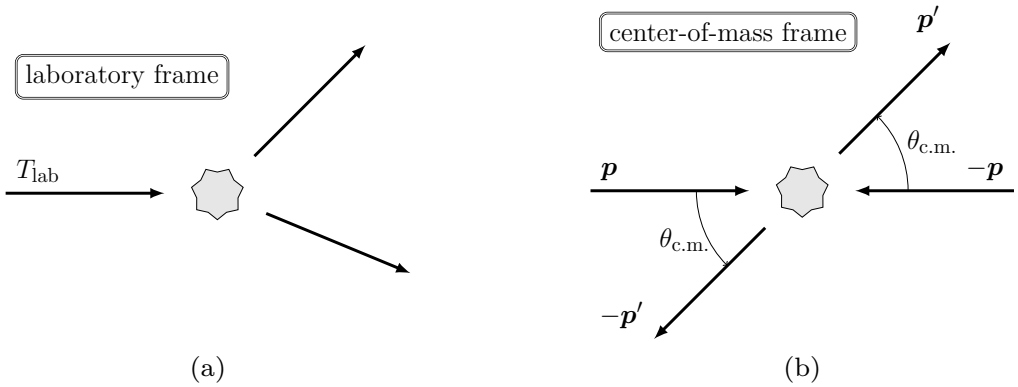

Figure 2.2: Illustration of *np* scattering see in the laboratory frame (a) and c.m. frame (b). $T_{\rm lab}$ denotes the laboratory scattering energy and $\boldsymbol{p}$ ($\boldsymbol{p}'$) the ingoing (outgoing) scattering momentum in the c.m. frame.

frames respectively. Two-nucleon scattering states can be described in the c.m. frame by the momentum basis states

$$|\boldsymbol{p}, s, m_s, t, m_t\rangle\,, \tag{2.5}$$

where $\boldsymbol{p}$ denotes the two-nucleon c.m. momentum. The quantum numbers of NN isospin ($\boldsymbol{T}$), angular momentum ($\boldsymbol{L}$) and spin ($\boldsymbol{S}$) are denoted t, ℓ and s respectively. The NN spin and isospin projections are denoted m_s and m_t. In this thesis, the following normalization is employed

$$\langle \boldsymbol{p}', s', m_s', t', m_t' | \boldsymbol{p}, s, m_s, t, m_t\rangle = (2\pi)^3\,\delta^3\left(\boldsymbol{p}' - \boldsymbol{p}\right)\delta_{s's}\delta_{m_s' m_s}\delta_{t't}\delta_{m_t' m_t}. \tag{2.6}$$

In the case of *np* scattering, $m_t = 0$ and $t = 0, 1$ are possible. The Pauli principle constrains the quantum numbers, ℓ, s, and t to obey $(-1)^{\ell+s+t} = -1$, which means that t is implicitly given by ℓ and s and can be dropped from the notation. Antisymmetric *np* partial-wave states are characterized by $|p, \ell, s, j\rangle$ where $p = |\boldsymbol{p}|$ and j is the quantum number associated with the total angular momentum operator, $\boldsymbol{J} = \boldsymbol{L} + \boldsymbol{S}$. Spectroscopic notation ${}^{2s+1}\ell_j$, where $\ell = 0, 1, 2, 3, \ldots$ is denoted $S, P, D, F, \ldots$ will be used to identify partial waves. An *np* scattering channel is characterized by the conserved quantum numbers s, j and $\Pi = (-1)^\ell$. If ℓ (ℓ') denotes the angular momentum in the ingoing (outgoing) state, then channels where $\ell' = \ell$ are referred to as uncoupled, and channels where $\ell' = j \pm 1$ and $\ell = j \pm 1$ are referred to as coupled.

Feynman diagrams and associated Feynman rules contributing to *np* scattering can be derived using $\mathcal{L}_{\rm eff}$ [14]. The chiral dimension, ν, of a given Feynman diagram can be calculated by counting the power of low energy scales appearing in the expression. It is given by

$$\nu = 4L - 2I_\pi - I_N + \sum_i d_i V_i, \tag{2.7}$$

(a) (b)

Figure 2.3: Feynman diagrams of order $\nu = 0$; contact interaction (a), and one-pion exchange (b). Solid lines represent nucleons and dashed lines pions.

where L is the number of loops, I_π (I_N) is the number of pion (nucleon) propagators and d_i is the number of derivatives/pion masses for vertex type i, and V_i is the number of vertices of type i. The PC resulting from Eq. (2.7) is sometimes referred to as naive dimensional analysis (NDA). Examples of diagrams with $\nu = 0$ ($\nu = 2$) are shown in Fig. 2.3 (Fig. 2.4).

The Lagrangians $\mathcal{L}^{(0)}_{NN}$ and $\mathcal{L}^{(2)}_{NN}$ consist of purely nucleon-nucleon interactions, and are thus called contact Lagrangians. These give rise to the following contact potentials in momentum space respectively,

$$V^{(0)}_{\rm ct}(\boldsymbol{p}',\boldsymbol{p}) \equiv \langle \boldsymbol{p}'|V^{(0)}_{\rm ct}|\boldsymbol{p}\rangle = C_S + C_T \boldsymbol{\sigma_1}\cdot\boldsymbol{\sigma}_2, \tag{2.8}$$

$$\begin{aligned} V^{(2)}_{\rm ct}(\boldsymbol{p}',\boldsymbol{p}) \equiv \langle \boldsymbol{p}'|V^{(2)}_{\rm ct}|\boldsymbol{p}\rangle &= C_1\boldsymbol{q}^2 + C_2\boldsymbol{k}^2 + \left(C_3\boldsymbol{q}^2 + C_4\boldsymbol{k}^2\right)\boldsymbol{\sigma_1}\cdot\boldsymbol{\sigma}_2 + \\ &+ C_5\left(-\frac{i(\boldsymbol{\sigma_1}+\boldsymbol{\sigma}_2)}{2}\cdot(\boldsymbol{q}\times\boldsymbol{k})\right) + \\ &+ C_6\left(\boldsymbol{\sigma}_1\cdot\boldsymbol{q}\right)\left(\boldsymbol{\sigma}_2\cdot\boldsymbol{q}\right) + C_7\left(\boldsymbol{\sigma}_1\cdot\boldsymbol{k}\right)\left(\boldsymbol{\sigma}_2\cdot\boldsymbol{k}\right), \end{aligned} \tag{2.9}$$

where $\boldsymbol{p}$ ($\boldsymbol{p}'$) is the c.m. momentum for one of the ingoing (outgoing) nucleons, $\boldsymbol{q} = \boldsymbol{p}' - \boldsymbol{p}$ and $\boldsymbol{k} = (\boldsymbol{p}' + \boldsymbol{p})/2$. The operators $\boldsymbol{\sigma}_i$ ($\boldsymbol{\tau}_i$) are the spin (isospin) operators for nucleon $i = 1, 2$. The potential $V^{(0)}_{\rm ct}$ will be projected into S-waves and $V^{(2)}_{\rm ct}$ into S- and P-waves[1] and will act as contact interactions (counterterms) in these channels. The LECs: $C_S,\ C_T,\ C_i,\ i = 1,\ldots,7$ parameterizing the interaction strengths will thus only act in partial waves with $\ell \leq 1$. This illustrates the fact that predictions in partial waves with $\ell > 1$ are entirely constrained by chiral symmetry up to this order. Similarly, the diagram in Fig. 2.3b can be calculated and the resulting one-pion-exchange (OPE) potential reads

$$V^{(0)}_{1\pi}(\boldsymbol{p}',\boldsymbol{p}) = -\frac{g_A^2}{4f_\pi^2}\frac{\left(\boldsymbol{\sigma}_1\cdot\boldsymbol{q}\right)\left(\boldsymbol{\sigma}_2\cdot\boldsymbol{q}\right)}{\boldsymbol{q}^2 + m_\pi^2}\left(\boldsymbol{\tau}_1\cdot\boldsymbol{\tau}_2\right), \tag{2.10}$$

where g_A is the axial coupling and f_π the pion decay constant.

[1] From the partial wave decomposition, it can be deduced that contact terms of order ν appear only in partial waves with $\ell \leq \nu/2$ [91].

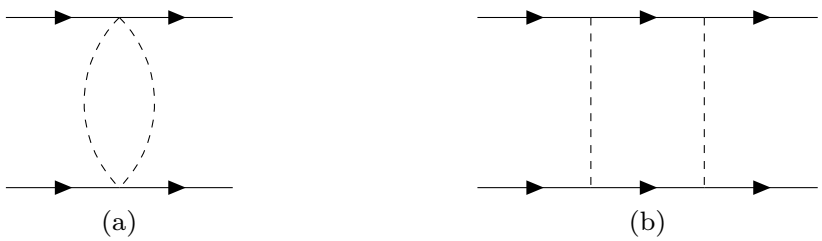

Figure 2.4: Examples of two-pion exchange Feynman diagrams with $\nu = 2$ that are irreducible (a) and reducible (b). Solid lines represent nucleons and dashed lines pions.

Equation (2.7) describes a perturbative PC where only a finite number of diagrams are present at each order, e.g., two at $\nu = 0$. This cannot be the full PC for describing nuclear physics since a perturbative PC provides no way of generating bound states. Bound states can only be generated non-perturbatively, and thus require some enhancement of diagrams with $\nu > 0$ necessitating a non-perturbative summation of an infinite number of diagrams at LO. In Ref. [15] Weinberg points out the presence of an infrared enhancement in diagrams that contain purely nucleonic intermediate states, i.e. diagrams that are two-nucleon reducible[2]. The infrared enhancement will mandate the promotion of certain parts of these diagrams from their order assigned by Eq. (2.7). In particular, there will be an infinite sum of diagrams at LO able to generate nuclear bound states.

The infrared enhancement can be illustrated by considering the two-nucleon reducible box diagram shown in Fig. 2.4b. The chiral dimension of this diagram is $\nu = 2$ according to Eq. (2.7), and it should therefore contribute at N^{2}LO in our notation. However, it can be shown [17, 91, 94, 95] that this box diagram can be broken into two parts

$$V^{(2)}_{2\pi,\mathrm{box}} = V^{\mathrm{it}}_{2\pi,\mathrm{box}} + V^{\mathrm{irr}}_{2\pi,\mathrm{box}}, \tag{2.11}$$

where $V^{\mathrm{irr}}_{2\pi,\mathrm{box}}$ is called the irreducible part and $V^{\mathrm{it}}_{2\pi,\mathrm{box}}$ the iterated part. The irreducible part will scale with the correct chiral dimension as shown in explicit calculations, in this case $\nu = 2$. The correct scaling for irreducible parts holds in general, and these diagrams can be evaluated and renormalized using, e.g., dimensional regularization.

The iterated part, however, will not follow the scaling assigned by Eq. (2.7) due to the infrared enhancement. This part of the two-pion exchange diagram

[2] A diagram is called two-nucleon *reducible* if two nucleon lines can be cut to form two new and allowed Feynman diagrams. Otherwise, the diagram is two-nucleon *irreducible*.

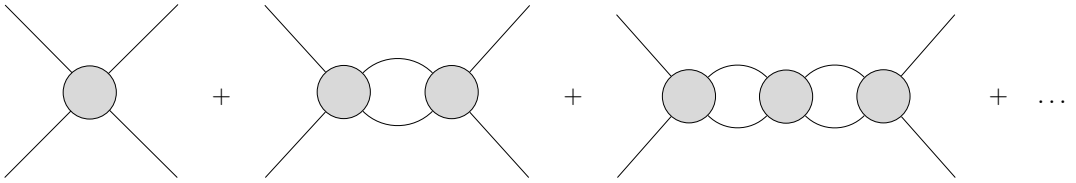

Figure 2.5: Diagrammatic representation of iterating the irreducible potential diagrams in the LS-equation (Eq. (2.16)). The ellipsis represents higher-order loops.

can be written as

$$V^{\mathrm{it}}_{2\pi,\mathrm{box}}(\boldsymbol{p}',\boldsymbol{p}) = \frac{g_A^2 m_N}{16 f_\pi^4}\left(3 - 2\boldsymbol{\tau}_1\cdot\boldsymbol{\tau_2}\right) \int \frac{d^3\boldsymbol{l}}{(2\pi)^3}\frac{(\boldsymbol{\sigma}_1\cdot\boldsymbol{q}_1)(\boldsymbol{\sigma}_2\cdot\boldsymbol{q}_1)}{\boldsymbol{q}_1^2+m_\pi^2}\frac{1}{\boldsymbol{p}^2-\boldsymbol{l}^2+i\epsilon}\frac{(\boldsymbol{\sigma}_1\cdot\boldsymbol{q}_2)(\boldsymbol{\sigma}_2\cdot\boldsymbol{q}_2)}{\boldsymbol{q}_2^2+m_\pi^2} \tag{2.12}$$

where the momentum transfers are $\boldsymbol{q}_1 = \boldsymbol{p}' + \boldsymbol{l}$ and $\boldsymbol{q}_2 = \boldsymbol{p} + \boldsymbol{l}$ [91]. This expression can be identified as the second-order term in the Born series for $V^{(0)}_{1\pi}$, namely

$$\langle \boldsymbol{p}'|\, V^{(0)}_{1\pi} G_0^+ V^{(0)}_{1\pi}\,|\boldsymbol{p}\rangle = \int \frac{d^3\boldsymbol{l}}{(2\pi)^3} V^{(0)}_{1\pi}(\boldsymbol{p}',\boldsymbol{l})\,\frac{m_N}{\boldsymbol{p}^2-\boldsymbol{l}^2+i\epsilon} V^{(0)}_{1\pi}(\boldsymbol{l},\boldsymbol{p})\,, \tag{2.13}$$

where

$$G_0^+ = \frac{m_N}{\boldsymbol{p}^2-\boldsymbol{l}^2+i\epsilon} \tag{2.14}$$

is the Schrödinger propagator in momentum space for an on-shell momentum $|\boldsymbol{p}|$. The neutron and proton masses are denoted m_n and m_p, respectively while $m_N = 2m_p m_n/(m_p+m_n)$ denotes the nucleon mass. The scaling of $V^{\mathrm{it}}_{2\pi,\mathrm{box}}$ in Eq. (2.12) is $Q^2(m_N/Q)$, with an enhancement of (m_N/Q) compared to $V^{\mathrm{irr}}_{2\pi,\mathrm{box}}$. To mandate the treatment of $V^{\mathrm{it}}_{2\pi,\mathrm{box}}$ at LO, which is necessary to be able to describe bound states, Ref. [15] concludes that m_N must be treated as larger than the breakdown scale $m_N \sim \Lambda_b^2/Q$. This can also be formulated as $(Q/m_N) = (Q/\Lambda_b)^2$, i.e. factors of (Q/m_N) are equivalent to two chiral orders. The enhancement of the iterated part will analogously appear for all two-nucleon reducible diagrams. With this enhancement, an infinite number of diagrams will contribute at LO, which can be treated by iterating potentials in the LS-equation to obtain the full amplitude.

WPC can now be summarized as follows. Potentials, $V^{(\nu)}$, are constructed according to the PC rule from Eq. (2.7):

$$V^{(\nu)} = \text{sum of all irreducible Feynman diagrams of order } \nu. \tag{2.15}$$

The full scattering amplitude is obtained by solving the LS-equation with $V^{(\nu)}$ to obtain the scattering T-operator[3]

$$T^{(\nu)} = V^{(\nu)} + V^{(\nu)} G_0^+ T^{(\nu)}. \tag{2.16}$$

Inserting the potential in the LS equation will take care of the summation of the enhanced part of diagrams with purely nucleonic intermediate states as can be seen by writing the Born series for Eq. (2.16)

$$T^{(\nu)} = V^{(\nu)} + V^{(\nu)} G_0^+ V^{(\nu)} + V^{(\nu)} G_0^+ V^{(\nu)} G_0^+ V^{(\nu)} + \dots. \tag{2.17}$$

The second term is seen to generate the expression in Eq. (2.13). This summation can be illustrated diagrammatically as shown in Fig. 2.5 where the blobs represent the potential $\left(V^{(\nu)}\right)$ and the internal lines correspond to Schrödinger propagators, G_0^+. When solving the LS-equation there is a need to introduce a momentum cutoff, Λ, to render results finite. The cutoff should be on the order of the breakdown scale or higher. An implicit assumption in WPC is that the solution of the LS-equation and associated loops does not bring any new cutoff dependence as opposed to that already taken care of by the renormalization of the irreducible parts of the pion loop diagrams. This assumption turns out to be false [60] which is a result of the potentials being singular, which will be elaborated upon in the next sub-section.

Singular potentials

Potentials derived from χEFT (and EFTs in general) tend to be singular. An attractive potential is singular near the origin if its short-range behavior in position space is $-\lambda/r^n$ where $n \geq 2$, and $\boldsymbol{r}$ is the relative position of the nucleons and $r = |\boldsymbol{r}|$. For the limiting case $n = 2$, the potential is singular only for sufficiently large $\lambda > 0$ [65, 96]. Particles interacting via attractive singular potentials will collapse into the origin $r = 0$ with increasing velocity. The reason why $n = 2$ is the turning point in non-relativistic quantum mechanics can be explained by the uncertainty principle, which implies the scaling $\sim 1/r^2$ for the kinetic energy in the vicinity of the origin. The singular potential, on the other hand, scales as $-\lambda/r^n, \quad n \geq 2$. For $n > 2$ (or $n = 2$ with sufficiently large λ) the kinetic energy term will be overcome by the potential for sufficiently small r. This leads to the total energy being unbounded from below which prohibits a well-defined solution to the Schrödinger equation.

The OPE potential is singular in some partial waves, which can be seen by

[3]Remember that the LS-equation is nothing more than the Schrödinger equation with scattering boundary conditions and knowing the T-operator is equivalent to knowing the full scattering state.

transforming the OPE potential in Eq. (2.10) to position space

$$V_{1\pi}^{(0)}(\boldsymbol{r}) = \int \frac{d^3\boldsymbol{q}}{(2\pi)^3}\, V_{1\pi}^{(0)}(\boldsymbol{p}', \boldsymbol{p}) = \tag{2.18}$$

$$= \frac{m_\pi}{12\pi}\left(\frac{g_A}{2f_\pi}\right)^2 \boldsymbol{\tau}_1 \cdot \boldsymbol{\tau}_2 \left[T(r) S_{12} + Y(r) \boldsymbol{\sigma}_1 \cdot \boldsymbol{\sigma}_2\right], \tag{2.19}$$

where $\boldsymbol{q} = \boldsymbol{p}' - \boldsymbol{p}$ is the momentum transfer and

$$S_{12} = 3\,(\boldsymbol{\sigma}_1 \cdot \hat{\boldsymbol{r}})\,(\boldsymbol{\sigma}_2 \cdot \hat{\boldsymbol{r}}) - \boldsymbol{\sigma}_1 \cdot \boldsymbol{\sigma}_2 \tag{2.20}$$

$$T(r) = \frac{e^{-m_\pi r}}{m_\pi r}\left[1 + \frac{3}{m_\pi r} + \frac{3}{(m_\pi r)^2}\right], \tag{2.21}$$

$$Y(r) = \frac{e^{-m_\pi r}}{m_\pi r}, \tag{2.22}$$

where $\hat{\boldsymbol{r}} = \boldsymbol{r}/r$. The short-range behavior in attractive spin-triplet partial waves will be singular due to $T(r) \sim 1/r^3$ for sufficiently small r. Whether specific partial waves are attractive or repulsive depends on the sign of the matrix element of the tensor operator $\boldsymbol{\tau}_1 \cdot \boldsymbol{\tau}_2 S_{12}$.

More generally, it can be shown that potentials with chiral order ν behave as $V^{(\nu)}(\boldsymbol{r}) \sim 1/r^{3+\nu}$ for $m_\pi r \ll 1$. Thus, potentials at higher chiral order are increasingly singular which is explained by the presence of higher powers of momenta in momentum space. These high powers in momentum space translate to high powers of r in the denominator in position space[4].

Singular potentials can be modified to possess a well-defined solution to the Schrödinger equation (or LS equation) by adding a local counterterm that absorbs the divergent short-range behavior [66, 98]. With this approach the singular potentials possess a well-defined limit when the momentum-space cutoff introduced in the LS equation is taken to infinity, $\Lambda \to \infty$[5], and predictions are independent of the arbitrary choice of Λ. This independence is not exact, but there can be a residual dependence on inverse powers of the cutoff that only vanishes in the infinite limit.

Nogga et al. [60] identified infinitely many spin-triplet partial waves of OPE which possess singular attraction. This is problematic in WPC since all the identified waves, except ${}^3S_1 - {}^3D_1$, do not have a counterterm at LO to counteract the singularities. This entails that the scattering amplitude obtained by solving Eq. (2.16) receives a Λ-dependence. This dependence can be absorbed by promoting counterterms with $\nu > 0$ to LO in the singular partial waves, and thus modifying WPC. The goal of modified PCs is to provide predictions independent of the cutoff, i.e., RG invariant, analogous to other EFTs [12]. However,

[4] Singular potentials and non-renormalizable field theories are tightly connected [97].

[5] Note that the $r \to 0$ limit in position space corresponds to the $\Lambda \to \infty$ limit in momentum space.

in practical calculations, only finite cutoffs can be explored and the cutoff independence can only be verified numerically. After cutoff independence is verified, you can of course choose a cutoff that is most appropriate for making calculations. Another possible way of dealing with singular potentials is to keep the cutoff finite in a range that proves to be phenomenologically successful, which is the approach used in WPC and advocated by Refs. [27, 42, 99–103]. We will not pursue the latter approach further in this work. Instead, we will proceed to analyze predictions of NN observables using a specific proposed modification of WPC, namely MWPC as formulated by Long and Yang.

2.2 Modified Weinberg Power Counting

As discussed in the previous section, attractive singular potentials require additional counterterms to fulfill RG invariance. A modified PC can be constructed using RG invariance as a guiding principle. A momentum cutoff (or more generally, any type of regulation) is nothing more than a way of splitting short-range physics between loops and LECs. Changing Λ in the LS equation will explicitly include more or less short-range physics, which can be compensated by adjusting the LECs. Thus, to obtain cutoff independence, i.e. RG invariance, it is central to include the necessary counterterms with associated LECs at each order. This is one of the primary tasks in developing an RG-invariant PC.

As demonstrated by Nogga et al. [60] there is an infinite number of singular attractive partial waves for the OPE potential, all of which would need a counterterm by the arguments in the previous section. This would call for an infinite number of parameters in the theory already at LO, which is problematic. However, a counterterm is only necessary for a singular potential if the potential is treated non-perturbatively. In fact, in partial waves with high enough orbital angular momentum, the interactions can be treated in perturbation theory.

Perturbative peripheral waves

It is a well-established fact that the strength of the nuclear interaction decreases as the quantum number of orbital angular momentum, ℓ, increases. This weakening effect eventually allows for a perturbative treatment, given sufficiently low scattering energies. More specifically, the OPE potential is perturbative in peripheral waves as explicitly studied in [94]. For sufficiently small scattering energies the singular short-range behavior of the potential is shielded by the centrifugal barrier, which adds an effective repulsive term to the potential that becomes stronger with increasing ℓ

$$V(\boldsymbol{r}) \to V(\boldsymbol{r}) + \frac{\ell(\ell+1)}{m_N r^2}. \tag{2.23}$$

The critical c.m. scattering momentum, $p_{\rm cr}$, below which OPE can be treated perturbatively was studied in Ref. [68] in various partial waves. It was shown that $p_{\rm cr} \gtrsim 400$ MeV for $\ell \geq 2$, which would imply that only partial waves with $\ell < 2$ need to be treated non-perturbatively up to $p \approx 400$ MeV and thus only a few attractive singular partial waves need to be provided with an additional counterterm. This avoids the need to introduce an infinite number of counterterms.

The approach of treating OPE exactly in partial waves with low ℓ and perturbatively in the remaining peripheral waves is sometimes referred to as partly perturbative pions. This can be seen as a modification to the early attempt of Refs. [62, 63] to include pions entirely perturbatively.

As argued in the previous section, higher-order chiral potentials tend to be increasingly singular. To obtain RG-invariant predictions beyond LO it was shown in Ref. [69][6] that the inclusion of sub-leading potentials must be done in distorted-wave perturbation theory, with the distortion made by the LO potential. As pointed out in Ref. [79], including corrections in perturbation theory has the advantage of providing an additional consistency check if corrections indeed are perturbative with respect to LO, as they should be. This consistency check can not be taken advantage of in the approach of solving for all potentials exactly as in WPC [79, 104].

To summarize, modified in MWPC means both promoted counterterms to lower chiral order than they are assigned by NDA as well as strictly perturbative inclusion of sub-leading orders. The MWPC follows the principles

(i) The chiral order of the irreducible parts of pion-exchange diagrams will be the same as for WPC dictated by NDA.

(ii) Counterterms are promoted to lower chiral order only if it is required to achieve cutoff independence (RG-invariance).

(iii) Corrections beyond LO are included perturbatively in distorted wave perturbation theory.

How perturbative computations of amplitudes in MWPC are implemented will be discussed in Chapter 3.

Potentials at LO

The modified expressions for the potentials used in this work are contained in Refs. [67, 75–77] and summarized in Paper II. As an example, we here look at how the LO potential is modified. In WPC the LO potential is in all partial

[6] This result is debated in Ref. [103] due to the existence of so-called exceptional points in the cutoff domain.

waves given by

$$V^{(0)}_{\rm WPC}(\boldsymbol{p}',\boldsymbol{p}) = -\frac{g_A^2}{4f_\pi^2}\frac{(\boldsymbol{\sigma}_1\cdot\boldsymbol{q})\,(\boldsymbol{\sigma}_2\cdot\boldsymbol{q})}{\boldsymbol{q}^2+m_\pi^2}\,(\boldsymbol{\tau}_1\cdot\boldsymbol{\tau}_2) + C_{^1S_0}\hat{P}_{^1S_0} + C_{^3S_1}\hat{P}_{^3S_1}, \quad (2.24)$$

where $\hat{P}_X$ (C_X) denotes the projector (LEC) for the indicated partial wave described by the LS-term $^{2s+1}\ell_j$. The potential is the sum of OPE and two non-derivative S-wave contact interactions coming from partial wave projection of the $\nu = 0$ contact potential in Eq. (2.8).

In MWPC, only the channels: $^1S_0$, $^3P_0$, $^1P_1$, $^3P_1$, $^3S_1$–$^3D_1$ and $^3P_2$–$^3F_2$ are treated non-perturbatively. In these channels, the LO potential reads

$$\begin{aligned} V^{(0)}_{\rm MWPC}(\boldsymbol{p}',\boldsymbol{p}) = &-\frac{g_A^2}{4f_\pi^2}\frac{(\boldsymbol{\sigma}_1\cdot\boldsymbol{q})\,(\boldsymbol{\sigma}_2\cdot\boldsymbol{q})}{\boldsymbol{q}^2+m_\pi^2}\,(\boldsymbol{\tau}_1\cdot\boldsymbol{\tau}_2) + C_{^1S_0}\hat{P}_{^1S_0} + \\ &+ C_{^3S_1}\hat{P}_{^3S_1} + \Big(D_{^3P_0}\hat{P}_{^3P_0} + D_{^3P_2}\hat{P}_{^3P_2}\Big)\,p'p. \end{aligned} \quad (2.25)$$

This potential has two more counterterms in singular triplet P-waves as compared to $V^{(0)}_{\rm WPC}$ (2.24). In channels that are treated perturbatively the potential at LO vanishes, i.e. $V^{(0)}_{\rm MWPC}(\boldsymbol{p}',\boldsymbol{p}) = 0$. For more detailed information about the potential expressions up to N^{3}LO, the reader is referred to Paper II.

Chapter 3

Predictions from Modified Weinberg Power Counting

In this chapter, we proceed to study predictions from MWPC for *np* scattering observables. We start with a brief overview of computing two-nucleon scattering observables in Section 3.1 and move on to the calibration of the unknown numerical values of the LECs in Section 3.2. Finally, selected results from Papers I and II are presented and discussed in Sections 3.3 and 3.4.

3.1 Neutron-Proton Scattering Observables

Studying *np* scattering is valuable in revealing information about unknown parameters in interaction potentials due to the abundance of experimental data. Indeed, there exists a database [105, 106] containing 3514 data points for several *np* scattering observables, covering laboratory scattering energies $T_{\text{lab}} = 10^{-6}$ MeV to 350 MeV. The highest scattering energy considered in this work will however be $T_{\text{lab}} = 200$ MeV. Figure 2.2 in Chapter 2 illustrates the kinematics of the two-nucleon scattering process. Note that the c.m. scattering angle, $\theta_{\text{c.m.}}$, is defined as the angle between the ingoing ($\boldsymbol{p}$) and outgoing ($\boldsymbol{p}'$) scattering momenta in the c.m. frame. This work focuses on the strong interaction in *np* scattering and isospin breaking as well as electromagnetic effects will be neglected.

Since nucleons are fermions with spin $\frac{1}{2}$, the Pauli matrices for nucleon $k = 1, 2$, denoted $\{\sigma_{kx}, \sigma_{ky}, \sigma_{kz}\}$ and $\sigma_{k0} \equiv \mathbb{1}$, form a basis for the respective one-particle spin density operator. A basis for the combined two-nucleon spin density operator, ρ, can be formed by considering tensor products of the basis states for each nucleon

$$S^{\mu} = \{\sigma_{1i} \otimes \sigma_{2j}\}, \quad i, j = 0, x, y, z. \tag{3.1}$$

giving the basis $\{S^\mu,\ \mu = 1, \ldots, 16\}$. The two-nucleon spin density operator can in this basis be written as

$$\rho = \frac{1}{4} \sum_{\mu=1}^{16} S^\mu \operatorname{Tr}\left(\rho S^\mu\right), \tag{3.2}$$

using the orthogonality relation $\operatorname{Tr}\left(S^\mu S^\lambda\right) = 4\delta_{\mu\lambda}$.

In the two-nucleon scattering process the spin density operator for the ingoing state, ρ_i, is by the interaction transformed to a spin density operator, ρ_f, for the outgoing state for a given scattering energy T_{lab} and a scattering angle $\theta_{\text{c.m.}}$. This can be summarized in the equation

$$\rho_f = \boldsymbol{M} \rho_i \boldsymbol{M}^\dagger, \tag{3.3}$$

where the 4-dimensional spin scattering matrix, $\boldsymbol{M}(T_{\text{lab}}, \theta_{\text{c.m.}})$, contains all dynamical information about the scattering process. Note that ρ_f is not necessarily properly normalized. The expectation value of a spin observable, $\mathcal{O}$, for the outgoing two-nucleon state is simply given by the Born rule for density operators

$$\langle \mathcal{O} \rangle_f = \frac{\operatorname{Tr}\left(\rho_f \mathcal{O}\right)}{\operatorname{Tr} \rho_f} = \frac{\operatorname{Tr}\left(\boldsymbol{M} \rho_i \boldsymbol{M}^\dagger \mathcal{O}\right)}{\operatorname{Tr}\left(\boldsymbol{M} \rho_i \boldsymbol{M}^\dagger\right)}. \tag{3.4}$$

However, this equation does not take the probability of getting ρ_f given ρ_i into account, i.e., the spin-averaged differential cross section which can be expressed as [107]

$$\frac{d\sigma}{d\Omega} = \frac{\operatorname{Tr}\left(\rho_f\right)}{\operatorname{Tr}\left(\rho_i\right)} = \frac{1}{4} \operatorname{Tr}\left(\boldsymbol{M} \boldsymbol{M}^\dagger\right). \tag{3.5}$$

Using Eq. (3.4) together with Eqs. (3.2) and (3.5) the expectation value for a basis state $\mathcal{O} = S^\mu$ can be expressed as

$$\langle S^\mu \rangle_f \times \frac{d\sigma}{d\Omega} = \operatorname{Tr}\left(\boldsymbol{M} \rho_i \boldsymbol{M}^\dagger S^\mu\right) = \frac{1}{4} \sum_{\lambda=1}^{16} \langle S^\lambda \rangle_i \operatorname{Tr}\left(\boldsymbol{M} S^\lambda \boldsymbol{M}^\dagger S^\mu\right), \tag{3.6}$$

where $\langle \cdot \rangle_i$ ($\langle \cdot \rangle_f$) denotes the expectation value with respect to ρ_i (ρ_f). Since both ρ_i and $\mathcal{O}$ have 16 possible basis states there are 256 possible spin-scattering experiments. Fortunately, it can be shown that parity conservation, the Pauli principle, and time reversal invariance limit this to 25 independent possibilities [108]. To calculate the various scattering observables we must solve the dynamics of the scattering process and construct $\boldsymbol{M}$. In the next section, we express $\boldsymbol{M}$ using the partial wave T-matrix for the *np* scattering process.

Scattering amplitudes at leading order

Two-nucleon potentials, for example the ones defined in Eq. (2.24) or Eq. (2.25), are naturally derived and expressed in the c.m. momentum basis, $|\boldsymbol{p}, s, m_s\rangle$, as illustrated in the previous chapter. The explicit relation between the partial wave states $|p, \ell, s, j\rangle$ introduced in Section 2.1 and this momentum basis reads

$$\langle p', \ell, s, j, m_j | \boldsymbol{p}, s, m_s \rangle = i^\ell \, (2\pi)^{3/2} \, \frac{\delta(p'-p)}{p^2} C^{jm_j}_{s\ell;m_s,m_j-m_s} Y^{*\ell}_{m_j-m_s}(\hat{\boldsymbol{p}}). \quad (3.7)$$

where $C^{j,m}_{j_1,j_2;m_1m_2}$ and $Y^\ell_m(\hat{\boldsymbol{p}})$ denote Clebsch-Gordan coefficients and spherical harmonics, respectively. The quantum number m_j associated with the projection of j can in Eq. (3.7) be set to zero by rotational invariance and will be dropped in the notation defining the partial wave states.

Matrix elements of the potential using the partial wave basis defined in Eq. (3.7) are written

$$V^{js}_{\ell'\ell}(p', p) = \langle p', \ell', s, j | V | p, \ell, s, j \rangle \, , \quad (3.8)$$

which indicates the conservation of both j and s, where the latter is a result of the Pauli principle in combination with parity invariance and assumed exact isospin symmetry. The partial-wave projection is in practice made in a helicity formalism to simplify calculations, following Ref. [109].

For a given potential V, the scattering T-matrix describing the quantum mechanical scattering amplitude is obtained as the solution to the LS-equation (see Eq. (2.16)) [110] which in the partial wave basis reads

$$T^{js}_{\ell'\ell}(p', p; p_0) = V^{js}_{\ell'\ell}(p', p) + \\ + \sum_{\ell''} \int_0^\infty dk \; k^2 \; V^{js}_{\ell'\ell''}(p', k) \frac{m_N}{p_0^2 - k^2 + i\epsilon} T^{js}_{\ell''\ell}(k, p; p_0). \quad (3.9)$$

The partial-wave form of the T-matrix is expressed completely analogous to Eq. (3.8). For an incoming neutron with kinetic energy $T_{\rm lab}$ the corresponding on-shell momentum, p_0, is given by

$$p_0 = \sqrt{\frac{m_p^2 T_{\rm lab}(2m_n + T_{\rm lab})}{(m_n + m_p)^2 + 2m_p T_{\rm lab}}}, \quad (3.10)$$

using relativistic kinematics. The on-shell elastic scattering amplitude is given by the matrix element $T^{js}_{\ell'\ell}(p_0, p_0; p_0)$ [107, 111]. The LS-equation can be solved numerically using, e.g., Gauss-Legendre quadrature [112, 113] to turn the integral equation into a linear system of equations. The typical number of discretization points needed for converged results is on the order of 100.

As mentioned in Section 2.1, the infinite momentum integral appearing in Eq. (3.9) needs to be regulated due to the infinite integration limit which renders

singular potentials divergent. The regulation is implemented by applying the transformation

$$V^{js}_{\ell'\ell}(p',p) \to f_\Lambda(p')V^{js}_{\ell'\ell}(p',p)f_\Lambda(p), \tag{3.11}$$

to the potentials, where common choices of the regulating function are

$$f_\Lambda(p) = \exp\left[-\frac{p^{2n}}{\Lambda^{2n}}\right], \tag{3.12}$$

with either $n = 2$ or $n = 3$ since they have a simple form and prove more numerically stable than a sharp cutoff [91]. One is of course free to choose any regulator function as long as it goes to zero sufficiently fast in the $\Lambda \to \infty$ limit. In Papers I and II we employ slightly different regulating functions to comply with earlier studies. The regulation effectively suppresses the high momentum components $p', p \gg \Lambda$ curing possible divergences in Eq. (3.9) and enables a numerical discretization on a finite interval. In Paper I we also use a so-called minimal relativity factor which makes the T-matrix satisfy a relativistic extension of the LS-equation [6, 114]. The minimal relativity factor can be implemented by modifying the regulating function as

$$f_\Lambda(p) \to f_\Lambda(p)\sqrt{\frac{m_N}{E(p)}}, \quad E(p) = \sqrt{m_N^2 + p^2}. \tag{3.13}$$

Minimal relativity is a percent-level effect for np scattering in the energy range that we consider ($T_{\rm lab} \lesssim 200$ MeV) and it was excluded from the analysis in Paper II.

With the partial-wave basis definition used in this thesis, the relation between the on-shell partial wave T- and S-matrix elements reads

$$S^{js}_{\ell'\ell}(p_0,p_0) = \delta_{\ell'\ell} - i\pi m_N p_0 T^{js}_{\ell'\ell}(p_0,p_0;p_0). \tag{3.14}$$

The partial-wave S-matrix in uncoupled channels (where $\ell' = \ell$) is a unitary one-by-one matrix that is trivially parameterized by a real phase shift, δ,

$$S^{js}_{\ell\ell} = e^{2i\delta}. \tag{3.15}$$

In coupled channels, the orbital angular momenta take the possible values $\ell' = j \pm 1$, $\ell = j \pm 1$, and the 2×2 unitary S-matrix can be parametrized in terms of three real phase shifts: δ_1, δ_2, and ϵ using the Stapp convention [115]

$$\begin{aligned} \boldsymbol{S}^{js} &= \begin{pmatrix} S^{js}_{\ell'=j-1,\ell=j-1} & S^{js}_{\ell'=j-1,\ell=j+1} \\ S^{js}_{\ell'=j+1,\ell=j-1} & S^{js}_{\ell'=j+1,\ell=j+1} \end{pmatrix} = \\ &= \begin{pmatrix} \cos(2\epsilon)e^{2i\delta_1} & i\sin(2\epsilon)e^{i(\delta_1+\delta_2)} \\ i\sin(2\epsilon)e^{i(\delta_1+\delta_2)} & \cos(2\epsilon)e^{2i\delta_2} \end{pmatrix}. \end{aligned} \tag{3.16}$$

The phase shifts can be expressed in terms of partial-wave scattering amplitudes $T^{js}_{\ell'\ell}(p_0, p_0; p_0)$ by inverting Eqs. (3.15) and (3.16) and using Eq. (3.14).

The unitarity of the partial-wave S-matrix relies on the scattering amplitude being calculated exactly using Eq. (3.9). In the next section, sub-leading chiral potentials will be added in perturbation theory, which adds corrections to $T^{js}_{\ell'\ell}$. This means that the unitarity of the partial-wave S-matrix will be perturbatively violated leading to slightly complex phase shifts if computed via Eq. (3.15) or Eq. (3.16).

Adding sub-leading orders using distorted-wave perturbation theory

Adding higher order corrections to the leading order potential can be formulated as adding an extra potential, $V_{\rm II}$, representing the sub-leading corrections. If V_I denotes the LO potential the Hamiltonian in the c.m. frame can be written

$$H = \frac{\boldsymbol{p}^2}{m_N} + V_{\rm I} + V_{\rm II}, \tag{3.17}$$

where $V_{\rm II}$ includes all the sub-leading corrections, which formally can be infinitely many. Denoting chiral potentials at order ν as $V^{(\nu)}$, $V_{\rm I}$ and $V_{\rm II}$ read

$$V_{\rm I} = V^{(0)}, \tag{3.18}$$

$$V_{\rm II} = \sum_{\nu=1}^{\infty} V^{(\nu)}. \tag{3.19}$$

The LO amplitude, $T^{(0)}$, is computed exactly by solving the LS-equation

$$T^{(0)} = V^{(0)} + V^{(0)} G_0^+ T^{(0)}, \tag{3.20}$$

for each partial wave. One approach to add the higher order corrections is to solve the LS-equation for the entire potential $V = V_{\rm I} + V_{\rm II}$. This is the approach taken in WPC, as discussed in Section 2.1. A central part to obtain RG-invariant results at orders beyond LO in the MWPC is, however, to include the corrections ($V_{\rm II}$) in perturbation theory, as discussed in Section 2.2. Since higher-order potentials in a sound PC should bring perturbative corrections, even if treated exactly, they should be amenable to a strict perturbative treatment. The difference between the exact and perturbative calculations should be a higher-order effect.

The starting point of including $V_{\rm II}$ perturbatively is to express the full scattering amplitude, T, from the Hamiltonian Eq. (3.17) as a distorted-wave Born (DWB)-series [116]

$$T = T^{(0)} + \Omega_-^\dagger V_{\rm II} \sum_{n=0}^{\infty} \left(G_1^+ V_{\rm II}\right)^n \Omega_+. \tag{3.21}$$

The Møller wave operators are given by

$$\Omega_+ = \mathbb{1} + G_0^+ T^{(0)}, \tag{3.22}$$

$$\Omega_-^\dagger = \mathbb{1} + T^{(0)} G_0^+, \tag{3.23}$$

which, acting upon plane-wave states, produce the corresponding distorted waves due to the presence of V_I. Furthermore, the propagator for the LO Hamiltonian is given by

$$G_1^+ = \Omega_+ G_0^+. \tag{3.24}$$

The DWB series is completely analogous to the Born series, but instead of expanding the amplitude around zero, one starts from the LO amplitude. Treating V_II as a perturbation and truncating the sum in Eq. (3.21) at $n = N$ produces the N:th order DWB approximation.

The perturbative potential corrections in Eq. (3.19) are in principle an infinite sum of higher-order chiral potentials. In this work, the highest order considered is $V^{(3)}$, which we refer to as N^{3}LO. Completely analogous to constructing the potentials from irreducible diagrams by counting the chiral order, the T-matrix corrections, $T^{(\nu)}$, are constructed from Eq. (3.21) by applying the same PC rules. Inserting Eq. (3.19) in Eq. (3.21), expanding both sums and organizing terms according to chiral orders give the expressions for the first, second, and third corrections with respect to the LO amplitude:

$$T^{(1)} = \Omega_-^\dagger V^{(1)} \Omega_+, \tag{3.25}$$

$$T^{(2)} = \Omega_-^\dagger \left(V^{(2)} + V^{(1)} G_1^+ V^{(1)} \right) \Omega_+, \tag{3.26}$$

$$\begin{aligned} T^{(3)} = \Omega_-^\dagger \Big(& V^{(3)} + V^{(2)} G_1^+ V^{(1)} + V^{(1)} G_1^+ V^{(2)} + \\ & + V^{(1)} G_1^+ V^{(1)} G_1^+ V^{(1)} \Big) \Omega_+. \end{aligned} \tag{3.27}$$

Note that these are the *corrections*. The full amplitude at, e.g., third order is given by the sum $T^{(0)} + T^{(1)} + T^{(2)} + T^{(3)}$. The above equations for the perturbative T-matrix corrections are solved numerically by projecting to the partial wave basis, in a fashion completely analogous to the solution of the LS-equation. The implementation and solution of Eqs. (3.25) to (3.27) are discussed in more detail in Paper II. The higher-order corrections to the T-matrix allow for the computation of higher-order phase shifts. In Paper II we describe how to perturbatively obtain corrections to the phase shifts in Eqs. (3.15) and (3.16) via a Taylor expansion. Perturbative corrections of phase shifts are also discussed in Refs. [77, 117].

It is now clear how we perturbatively obtain T-matrix amplitudes from a given set of chiral potentials $\{V^{(\nu)}\}_{\nu \leq 3}$. The construction of the spin-scattering matrix can now be revisited, which is the final step to computing scattering observables.

Computing observables from partial-wave amplitudes

The partial wave S-matrix for a given on-shell momentum, p_0, is constructed by summing the on-shell T-matrix contributions up to the given order and using Eq. (3.14) yielding

$$S^{(\nu)js}_{\ell'\ell}(p_0,p_0) = \delta_{\ell'\ell} - i\pi m_N p_0 \times \left[T^{(0)js}_{\ell'\ell}(p_0,p_0;p_0) + \cdots + T^{(\nu)js}_{\ell'\ell}(p_0,p_0;p_0)\right]. \tag{3.28}$$

For $\nu \geq 1$, the partial wave T-matrix amplitudes, $T^{(\nu)js}_{\ell'\ell}$, are computed perturbatively as described in the last section, and the resulting partial-wave S-matrix is not unitary. Non-unitarity is a common feature in all types of perturbative calculations. However, some care must be taken when calculating observables. For example, calculating the total cross section in np scattering using the optical theorem [110] is no longer exact. Instead, the discrepancy between the result using the optical theorem and integration of the differential cross section will give a quantitative measure of the unitary breaking. Since the sum for $\nu \to \infty$ in Eq. (3.28) should give a unitary amplitude, the unitary breaking at some order ν should be a $(\nu+1)$-order effect which should be reflected in the unitary breaking being smaller at higher orders. Consequences of the non-unitary amplitudes are something we discuss in more detail in Paper II.

The matrix elements of the spin-scattering matrix, $\boldsymbol{M}$, can be expressed in terms of partial-wave scattering amplitudes as [107, 118, 119]

$$M^{s}_{m'_s m_s}(p_0,\theta_{\text{c.m.}},\phi) = \frac{\sqrt{4\pi}}{2ip_0}\sum_{j,\ell,\ell'} i^{\ell-\ell'}(2j+1)\sqrt{2\ell+1} \times \begin{pmatrix} \ell' & s & j \\ m_s - m'_s & m'_s & -m_s \end{pmatrix}\begin{pmatrix} \ell & s & j \\ 0 & m_s & -m_s \end{pmatrix} \times Y^{\ell'}_{m_s-m'_s}(\theta_{\text{c.m.}},\phi)\left(S^{(\nu)js}_{\ell'\ell}(p_0,p_0) - \delta_{\ell'\ell}\right). \tag{3.29}$$

for the total spin (s) and its projections in the ingoing state (m_s) and outgoing state[1] (m'_s). The angles $\theta_{\text{c.m.}} \in [0,\pi]$ and $\phi \in [0,2\pi)$ are the polar and azimuthal scattering angles, respectively. The latter can be set to zero by cylindrical symmetry and is from now on omitted. Note that this sum implicitly takes the Pauli principle into account since only proper antisymmetrized partial-wave states are included. The matrices in Eq. (3.29) are Wigner $3j$-symbols[2] and

[1] Since T_{lab} and p_0 are equivalent by Eq. (3.10) either one can be used to indicate the energy dependence of M-matrix elements.

[2] The relation between Clebsch-Gordan coefficients and Wigner $3j$-symbol is [110].

$$C^{j,m}_{j_1,j_2;m_1m_2} \equiv \langle j_1,j_2;m_1m_2|j_1j_2;jm\rangle = (-1)^{j_1-j_2+m}\sqrt{2j+1}\begin{pmatrix} j_1 & j_2 & j \\ m_1 & m_2 & -m \end{pmatrix}.$$

the sum over j, ℓ', and ℓ is taken with respect to the spin-coupling rules and truncated at some $j_{\max}$. One generally needs higher $j_{\max}$ for larger T_{lab}. In np scattering without electromagnetic effects, $j_{\max} \approx 15$ is more than enough to obtain convergence up to $T_{\text{lab}} = 200$ MeV,

Using the elements given in Eq. (3.29) the $\boldsymbol{M}$ matrix can be constructed. In the uncoupled NN spin basis $\{|m_1, m_2\rangle\,,\ m_1 = \pm\frac{1}{2},\ m_2 = \pm\frac{1}{2}\}$[3] given by the spin projections of the respective nucleon, the $\boldsymbol{M}$ matrix can be written in terms of a Kronecker product as

$$\boldsymbol{M} = \begin{pmatrix} M^1_{11} & \frac{1}{\sqrt{2}}M^1_{10} & \frac{1}{\sqrt{2}}M^1_{10} & M^1_{1-1} \\ \frac{1}{\sqrt{2}}M^1_{01} & \frac{1}{2}\left(M^0_{00} + M^1_{00}\right) & \frac{1}{2}\left(-M^0_{00} + M^1_{00}\right) & \frac{1}{\sqrt{2}}M^1_{0-1} \\ \frac{1}{\sqrt{2}}M^1_{01} & \frac{1}{2}\left(-M^0_{00} + M^1_{00}\right) & \frac{1}{2}\left(M^0_{00} + M^1_{00}\right) & \frac{1}{\sqrt{2}}M^1_{0-1} \\ M^1_{-11} & \frac{1}{\sqrt{2}}M^1_{-10} & \frac{1}{\sqrt{2}}M^1_{-10} & M^1_{-1-1} \end{pmatrix}. \tag{3.30}$$

Given the $\boldsymbol{M}$ matrix, expressions for some relevant spin-observables can be formed using Eq. (3.6). The simplest observation in the final state of the scattering process is to ignore the spin polarization, corresponding to the observable $\mathcal{O} = \mathbb{1}_1 \otimes \mathbb{1}_2$. Analogously, the simplest initial density operator representing an average over the possible initial spin polarization is given by $\rho_i = (\mathbb{1}_1 \otimes \mathbb{1}_2)/4$. Using Eq. (3.6) this setup reduces to the spin-averaged differential cross section already defined in Eq. (3.5). Other important classes of observables are spin-polarization and spin-correlation observables. Examples of these are P_b and A_{yy}, defined as

$$P_b \times \frac{d\sigma}{d\Omega} = \frac{1}{4}\,\mathrm{Tr}\big\{\boldsymbol{M}\,(\boldsymbol{\sigma}_1 \cdot \hat{\boldsymbol{n}})\,\boldsymbol{M}^\dagger\big\}, \tag{3.31}$$

$$A_{yy} \times \frac{d\sigma}{d\Omega} = \frac{1}{4}\,\mathrm{Tr}\big\{\boldsymbol{M}\big[\,(\boldsymbol{\sigma}_1 \cdot \hat{\boldsymbol{n}}) \otimes (\boldsymbol{\sigma}_2 \cdot \hat{\boldsymbol{n}})\,\big]\boldsymbol{M}^\dagger\big\}, \tag{3.32}$$

where $\hat{\boldsymbol{n}}$ is normal to the scattering plane, which by convention is chosen as the xz-plane [108]. The dimensionless observable P_b gives a measure of the asymmetry in the differential cross section induced by polarizing one nucleon. Analogously, the dimensionless observable A_{yy} gives a measure of the spin-correlation induced by the scattering process.

[3] The uncoupled basis $|m_1, m_2\rangle$ is related to the coupled spin basis $|s, m_s\rangle$ as

$$|s, m_s\rangle = \sum_{m_1, m_2} C^{s,m_s}_{1/2,1/2;m_1 m_2}\,|m_1, m_2\rangle\,.$$

3.2 Connecting Theory and Experiment

Having looked at both the construction of interaction potentials from χEFT in Chapter 2 and how to numerically compute scattering observables at each chiral order in Section 3.1, it is time to consider the connection between theory and experiment. This connection is of course important for evaluating the validity of the theoretical description, but also central for calibrating the unknown LECs appearing in the χEFT potentials.

The Bayesian approach

In later years Bayesian inference has been increasingly used in nuclear theory, and in particular dealing with interactions from EFT [33–38], expanding on early developments [32]. Much of this work is analogously applied in perturbative QCD [120]. As discussed in Section 2.1, a strength of the EFT approach is the naturally arising expression for the EFT model error. We will now explicitly look at how this model error (also referred to as the EFT truncation error) arises and how it naturally can be incorporated in the analysis of the link between theory and experiment using a Bayesian approach.

The power of using a Bayesian approach is twofold. Firstly, the model parameters (LECs) are seen as random variables, and hence are characterized by a probability distribution and not just a set of some "optimal" values. This gives a natural way of propagating errors. Secondly, there is the transparency of assumptions through the prior probability distribution, which can include various physical principles, such as expected naturalness.

The assumed χEFT expansion for an observable, y, is

$$y = y_0 \sum_{n=0}^{\infty} c_n \left(\frac{Q}{\Lambda_b}\right)^n, \tag{3.33}$$

where y_0 is a natural scale of the observable, $\{c_n\}_{n\geq 0}$ are dimensionless expansion coefficients and Q/Λ_b is the EFT expansion parameter [34]. Note that $c_1 = 0$ in WPC by parity and time-reversal symmetry [91]. Truncating this sum gives the theoretical prediction at order ν, and a remaining term

$$y = y_{\text{th}}^{(\nu)} + y_0 \sum_{n=\nu+1}^{\infty} c_n \left(\frac{Q}{\Lambda_b}\right)^n. \tag{3.34}$$

The remaining term naturally characterizes the EFT truncation error at order ν

$$\delta y_{\text{th}} = y_0 \sum_{n=\nu+1}^{\infty} c_n \left(\frac{Q}{\Lambda_b}\right)^n. \tag{3.35}$$

At order ν, the leading EFT truncation error is proportional to $(Q/\Lambda_b)^{\nu+1}$ and captures the fact that this low-energy EFT is more accurate at low energies ($\sim m_\pi$) rather than high ($\sim \Lambda_b$).

The relation between experimental data, $y_{\rm exp}$, and a theoretical prediction, $y_{\rm th}^{(\nu)}$, of an observable can be modeled as

$$y_{\rm exp} = y_{\rm th}^{(\nu)} + \delta y_{\rm th} + \delta y_{\rm exp}, \tag{3.36}$$

where $\delta y_{\rm th}$, and $\delta y_{\rm exp}$ are random variables representing the theoretical and experimental errors respectively. The experimental error is commonly modeled as a normal distribution with a standard deviation $\sigma_{\rm exp}$ as

$$\text{pr}\left(\delta y_{\rm exp}\right) = \mathcal{N}\left(0, \sigma_{\rm exp}^2\right), \tag{3.37}$$

where $\mathcal{N}\left(\mu, \sigma^2\right)$ denotes a normal distribution with mean μ and variance σ^2 and $\text{pr}\left(\cdot\right)$ denotes the probability density function (pdf). Moreover, the theory error can be calculated quantitatively using some prior assumptions on the coefficients $\{c_n\}_{n>\nu}$ giving a typical distribution

$$\text{pr}\left(\delta y_{\rm th}\right) = \mathcal{N}\left(0, \sigma_{\rm th}^2\right), \tag{3.38}$$

where the variance $\sigma_{\rm th}^2$ depends on the assumptions being made. As an example, in Paper I we follow Ref. [34] where $\{c_n\}_{n>\nu}$ are assumed to be independent and identically distributed (i.i.d) as $\mathcal{N}\left(0, \bar{c}^2\right)$. This gives

$$\sigma_{\rm th}^2 = \frac{y_0^2 \bar{c}^2 \left(\frac{Q}{\Lambda_b}\right)^4}{1 - \left(\frac{Q}{\Lambda_b}\right)^2}, \tag{3.39}$$

where the parameter $\bar{c}$ governs the variance of $\{c_n\}_{n>\nu}$. In the above model, $c_1 = 0$ by parity and time-reversal symmetry [91]. The likelihood of observing a given experimental datum can be expressed as

$$\text{pr}\left(y_{\rm exp}|\boldsymbol{\alpha}^{(\nu)}, I\right) = \mathcal{N}\left(y_{\rm th}^{(\nu)}\left(\boldsymbol{\alpha}^{(\nu)}\right), \sigma_{\rm th}^2 + \sigma_{\rm exp}^2\right), \tag{3.40}$$

assuming independent experimental and theoretical errors. Here, $\boldsymbol{\alpha}^{(\nu)}$ denote the LECs present in the potentials up to order ν and I encapsulates additional information and assumptions included in the error models. As an example, for the LO potential in Eq. (2.25) we define $\boldsymbol{\alpha}^{(0)} = (C_{^1S_0}, C_{^3S_1}, D_{^3P_0}, D_{^3P_2})$.

Given a data set $D = \{y_{\rm exp}\}$ of measured observables, the likelihood for the data set can be converted to a posterior probability density for the LECs using Bayes' rule

$$\text{pr}\left(\boldsymbol{\alpha}^{(\nu)}|D, I\right) = \frac{\text{pr}\left(D|\boldsymbol{\alpha}^{(\nu)}, I\right) \cdot \text{pr}\left(\boldsymbol{\alpha}^{(\nu)}|I\right)}{\text{pr}\left(D|I\right)}. \tag{3.41}$$

Here, $\text{pr}\left(\boldsymbol{\alpha}^{(\nu)}|I\right)$ denotes the *prior* and $\text{pr}\left(D|I\right)$ the *model evidence* which here serves as a normalization factor. Using Eq. (3.41) one naturally incorporates the prior information of the naturalness of LECs through $\text{pr}\left(\boldsymbol{\alpha}^{(\nu)}|I\right)$. The likelihood for the full data set, $\text{pr}\left(D|\boldsymbol{\alpha}^{(\nu)}, I\right)$, can be constructed as the product of the individual likelihoods in Eq. (3.40) under the assumption that the model errors are independent, which is the approach taken in Paper I. It is possible to relax the assumption of independence and describe the model errors collectively using a covariance matrix, Σ_{th}. This approach is explored in Refs. [36, 121] but not considered in this work.

Evaluating Eq. (3.41) at LO for varying cutoffs Λ is the main focus of Paper I. This is done using a Bayes linear approach known as history matching [50, 122–124], and Markov chain Monte Carlo (MCMC) sampling. The resulting pdfs $\text{pr}\left(\boldsymbol{\alpha}^{(\nu)}|D, I\right)$ quantify the uncertainties of the LECs stemming from the various sources of error. In particular, we find that including the model-error information provides a more robust inference since it effectively weights the information content in the experimental data, where low-energy data is expected to give more information about the EFT.

Having a probabilistic representation of the LECs allows for properly propagating uncertainties to predictions via marginalization

$$\text{pr}\left(y|D, I\right) = \int d\boldsymbol{\alpha}^{(\nu)}\ \text{pr}\left(y|\boldsymbol{\alpha}^{(\nu)}, D, I\right) \text{pr}\left(\boldsymbol{\alpha}^{(\nu)}|D, I\right), \tag{3.42}$$

where $\text{pr}\left(y|D, I\right)$ is called the posterior predictive distribution (ppd) for the observable y. When evaluating the above integral we can incorporate the EFT truncation error in the model prediction via

$$\text{pr}\left(y|\boldsymbol{\alpha}^{(\nu)}, D, I\right) = \mathcal{N}\left(y_{\text{th}}^{(\nu)}\left(\boldsymbol{\alpha}^{(\nu)}\right), \sigma_{\text{th}}^2\right). \tag{3.43}$$

The model error can also be excluded by using a delta distribution

$$\text{pr}\left(y|\boldsymbol{\alpha}^{(\nu)}, D, I\right) = \delta\left(y - y_{\text{th}}^{(\nu)}\left(\boldsymbol{\alpha}^{(\nu)}\right)\right), \tag{3.44}$$

which corresponds to only propagating the LEC uncertainty. The ppd quantifies the model prediction for an observable as a pdf, given the calibration data, D, and assumptions I.

This section has shown a specific example of how the relation between experiment and theory can be used in χEFT to infer LECs and make predictions. In particular, we saw how the model error term arises and how it can be included in the inference of LECs through Bayes' rule. The two following sections summarize some of the main results of Paper I and Paper II.

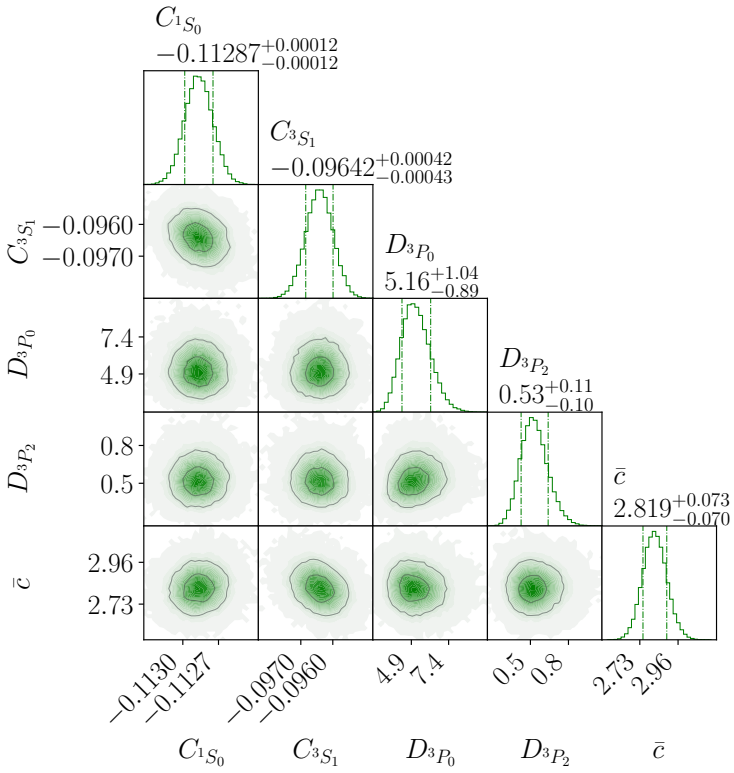

Figure 3.1: Posterior pdf for the parameters $\boldsymbol{\theta} = \left(\boldsymbol{\alpha}^{(0)}, \bar{c}\right)$ for cutoff $\Lambda = 450$ MeV. The units of the LECs are 10^4 GeV^{-2} and 10^4 GeV^{-4} for the S- and P-waves respectively. The median and the 68% equal-tailed credible interval are indicated for the univariate marginal pdfs.

3.3 Bayesian Analysis of MWPC at LO

In Paper I we performed a thorough Bayesian analysis of the LEC values of the LO potential in MWPC conditioned on *np* scattering data. The main motivation was to test the hypothesis of overfitted LECs put forward by Yang et al. [83] as a possible explanation for MWPC predictions failing in nuclei beyond $A = 4$, as discussed in the introduction. The LECs used in Ref. [83] were inferred from phase shifts, which possibly induced sufficient overfitting to render unphysical predictions of nuclear observables. We investigated the calibration of LECs at LO in MWPC, conditioning the inference on *np* scattering data as well as incorporating the EFT model error. Since we used a relatively weakly informed error model, spin-polarization observables were not included in the inference.

When doing the LEC inference we varied the cutoff in the LS-equation in a rather large interval ranging from $\Lambda = 400$ MeV to $\Lambda = 4000$ MeV. The singular nature of the LO potential induces limit-cycle-like behavior and spurious bound states which makes the LEC values change rapidly as a function of the cutoff. The rapid variation of LECs posed challenges in the initialization of MCMC chains for the large span of cutoffs. We mitigated this problem by employing history matching to efficiently identify relevant initialization domains for the LECs.

Figure 3.1 shows the posterior pdf for the LEC-values for the cutoff $\Lambda = 450$ MeV. This pdf also includes $\bar{c}$, parametrizing the size of the EFT truncation error (3.39), which we also inferred from the data. Given the posterior pdf for the LECs, we computed ppds for both phase shifts and observables. Figure 3.2 shows the ppd for phase shifts compared to the empirical partial wave analysis in Ref. [81] and the study in Ref. [83]. In particular, it was demonstrated that the phase shifts in some P-waves are quite different in our analysis, which confirms that the inference procedure highly impacts the final results.

Moreover, we computed ppds for scattering observables and the deuteron ground state energy confirming that our inferred LECs indeed produced a satisfactory description of *np* observables and that the results were independent of the cutoff. The results of this study demonstrated that using scattering observables rather than phase shifts as calibration data has a large impact on the resulting LECs, and thus on the resulting predictions.

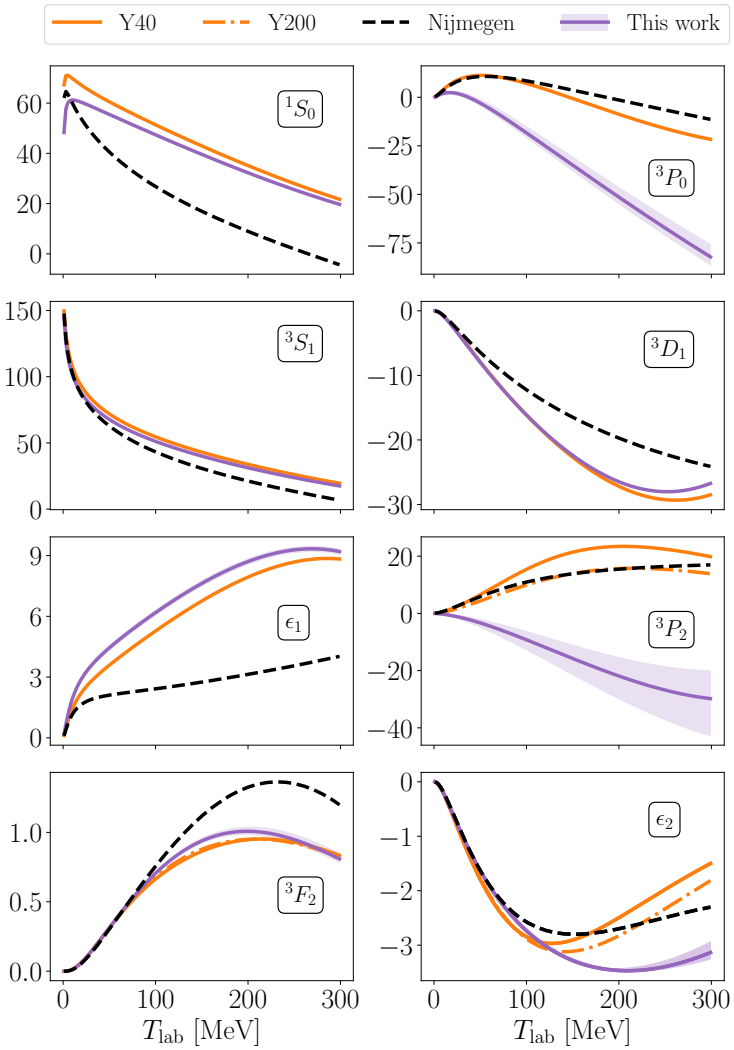

Figure 3.2: Predicted phase shifts (in degrees) with $\Lambda = 450$ MeV represented by the median of the ppd (solid purple line) and the 95% equal-tailed credible interval (purple band). Note that the EFT error is not included. Our results are compared to the phase shifts of [83] and the Nijmegen partial-wave analysis [81]. The labels Y40 and Y200 indicate the two types of fits that were done by [83] in the $^3P_2$–$^3F_2$ channel; renormalizing the corresponding LECs to reproduce the $^3P_2$ phase shifts at $T_{\text{lab}} = 40$ MeV and $T_{\text{lab}} = 200$ MeV, respectively.

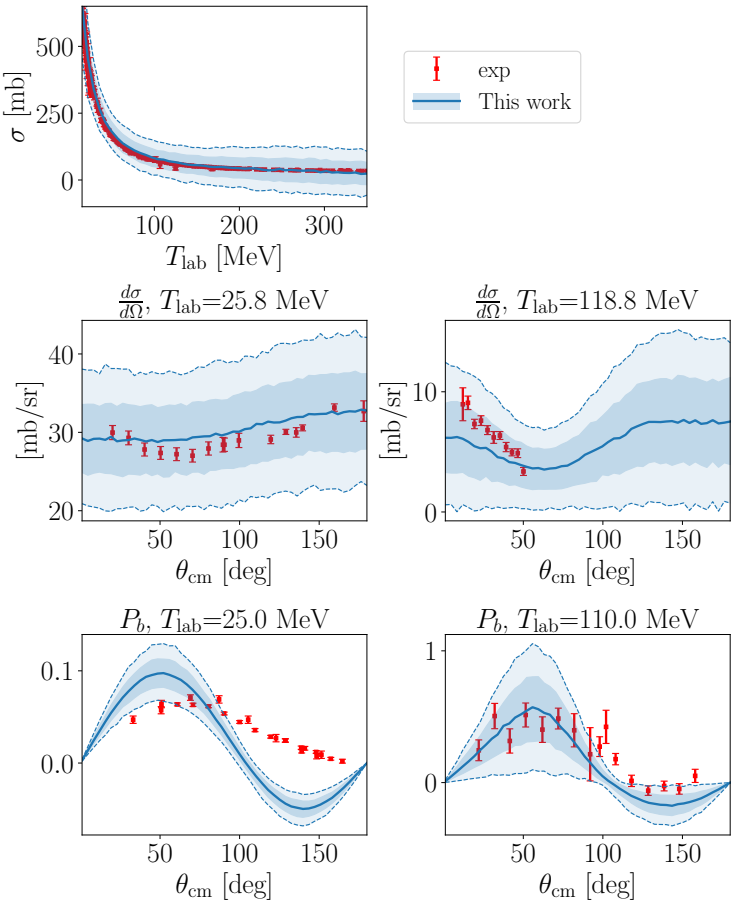

Figure 3.3: Median (solid blue line) of the ppds for selected np scattering observables using MWPC at LO with a cutoff $\Lambda = 450$ MeV. The EFT error is included. Shaded dark and light blue bands represent 68% and 95% equal-tailed credible intervals, respectively. Experimental data (exp) is from Refs. [105, 106].

3.4 Predictions from MWPC up to N^{3}LO

In Paper II, we move on to computing *np* scattering observables in perturbation theory up to N^{3}LO in MWPC. This work aims to establish a computational framework and to make a first attempt at quantitatively describing *np* scattering observables in MWPC. In this first analysis, we employ a simpler method to infer the LEC values compared to Paper I. We follow the procedure used in Refs. [75–77] and infer the LEC values by reproducing phase shifts from Ref. [81] at certain energies. Using the method described in the previous sections in this chapter we compute *np* scattering observables up to N^{3}LO.

The most important results of Paper II are summarized in Fig. 3.4. The figure shows the scattering observables $\frac{d\sigma}{d\Omega}$, P_b and A_{yy}, defined in Eqs. (3.5), (3.31) and (3.32) respectively, for a selection of scattering energies in the interval $T_{\rm lab} = 10$ to $T_{\rm lab} = 100$ MeV. The bands in the figure are defined by results computed at two different momentum cutoffs, $\Lambda = 500$ MeV and $\Lambda = 2500$ MeV. While these bands lack statistical meaning, they still provide a useful indication of the anticipated size of the model error. A satisfactory order-by-order description of data is observed, which confirms that a perturbative description of scattering observables up to scattering energies $T_{\rm lab} \lesssim 100$ MeV is possible.

Furthermore, we also compute the total cross section for *np* scattering using two methods; (i) the optical theorem and (ii) integrating the differential cross section. We use the difference between these two calculations as a way of assessing the unitary breaking in the perturbative calculation. As expected, we observe more unitary breaking at the lower chiral orders.

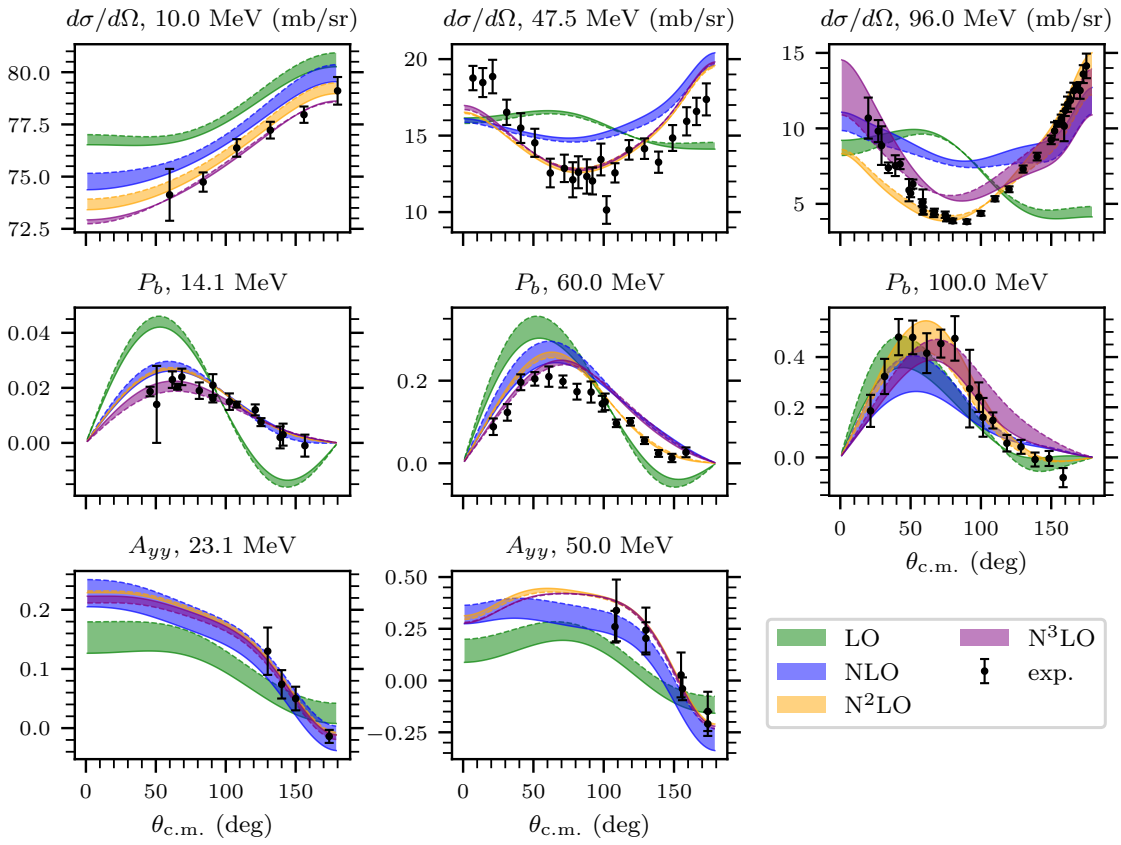

Figure 3.4: A selection of neutron-proton scattering observables in the energy interval $T_{\text{lab}} = 10$ to 100 MeV. Experimental data (exp) taken from Refs. [105, 106]. The bands indicate cutoff variation between $\Lambda = 500$ MeV (indicated with a dashed line) and $\Lambda = 2500$ MeV (solid line).

Chapter 4

Summary and Outlook

Describing atomic nuclei from first principles using the Schrödinger equation is a task that contains multiple challenging elements. In this thesis, the focus has been on describing the nuclear interaction from χEFT in the MWPC proposed by Long and Yang. The OPE potential entering at order $\nu = 0$ turns out to have a central role, which is quite interesting from a historical perspective. The pion-exchange description from Yukawa is still highly relevant, but here it appears in the modern light of χEFT.

The problems of lacking RG-invariance in WPC, stemming from singular potentials, have been known for more than two decades and have spurred several proposals for new ways of doing the PC. In this work, we have analyzed the proposal by Long and Yang by computing *np* scattering observables to N^{3}LO and by conducting a detailed Bayesian inference study of the LO potential including its truncation error.

In the Bayesian study of the LO interaction, presented in Paper I, we address how to properly calibrate LECs from data with models of the EFT truncation error. It is clear from the analysis in Paper I that the inference procedure has a large impact on the resulting posteriors of the LECs, and that the inclusion of EFT truncation errors has a significant role in mitigating overfitting. However, the inference method employed in Paper I can still be improved. The weakly informed error model made it challenging to include spin-polarization observables in the inference. The results, however, demonstrate that a sound inference procedure including dominant sources of uncertainty might provide a solution to the challenge of obtaining realistic predictions for ground-state energies observed in Ref. [83].

In Paper II we studied how well MWPC can describe *np* scattering observables up to N^{3}LO. The predicted cross sections exhibit an order-by-order convergence consistent with expectations. The observed convergence pattern hints that the breakdown of the perturbative expansion might be as low as

$T_{\rm lab} = 100$ MeV in its current formulation. Further studies are warranted and will hopefully reveal more information about how well the perturbative expansion is performing and guide the construction of the LO potential.

The Bayesian inference analysis at LO would be greatly improved by employing an error model informed by the convergence pattern of observables. For this, computations at higher orders are essential. The results in Paper II demonstrate that such a program can be pursued.

The next step is therefore to extend and improve the Bayesian inference of LECs performed in Paper I to (at least) N^{3}LO in the *np* sector. However, inference beyond LO based on perturbative calculations of *np* scattering presents several challenges compared to non-perturbative calculations. Perturbative calculations (*i*) include more LECs, (*ii*) might induce cancellations and correlations between contributions at different orders, and (*iii*) are computationally more costly.

A key question to address in future work is how MWPC potentials describe properties of nuclei with mass-number $A > 2$. For this, there is a need to develop efficient many-body methods for computing bound state properties in MWPC to high chiral orders.

As stressed in this thesis, the LO contribution to the nuclear potential is highly important in perturbative calculations since it is the foundation upon which all subsequent orders rest. There are several indications that the present LO descriptions fail to capture the relevant low-energy dynamics of the nuclear force. Consequently, several recent works have addressed the question of how LO can be modified [125–127]. The perturbative framework of MWPC, presented in this thesis, is a valuable starting point for continued efforts to address the possible modifications of the PC used in χEFT.

Bibliography

[1] E. Rutherford, "The scattering of alpha and beta particles by matter and the structure of the atom", Phil. Mag. Ser. 6 **21**, 669–688 (1911).

[2] J. Chadwick, "The Existence of a Neutron", Proc. Roy. Soc. Lond. A **136**, 692–708 (1932).

[3] E. Wigner and F. Seitz, "On the Constitution of Metallic Sodium", Phys. Rev. **43**, 804–810 (1933).

[4] H. Yukawa, "On the Interaction of Elementary Particles I", Proc. Phys. Math. Soc. Jap. **17**, 48–57 (1935).

[5] H. A. Bethe, "Theory of the Effective Range in Nuclear Scattering", Phys. Rev. **76**, 38–50 (1949).

[6] R. Machleidt, "The meson theory of nuclear forces and nuclear structure", in *Advances in nuclear physics*, edited by J. W. Negele and E. Vogt (Springer US, Boston, MA, 1989), pp. 189–376.

[7] D. J. Gross, "The discovery of asymptotic freedom and the emergence of QCD", Proc. Nat. Acad. Sci. **102**, 9099–9108 (2005).

[8] S. Weinberg, "Phenomenological Lagrangians", Physica A **96**, edited by S. Deser, 327–340 (1979).

[9] H. W. Hammer, S. König, and U. van Kolck, "Nuclear effective field theory: status and perspectives", Rev. Mod. Phys. **92**, 025004 (2020), arXiv:1906.12122 [nucl-th].

[10] E. Epelbaum, H.-W. Hammer, and U.-G. Meissner, "Modern Theory of Nuclear Forces", Rev. Mod. Phys. **81**, 1773–1825 (2009), arXiv:0811.1338 [nucl-th].

[11] J Gasser and H Leutwyler, "Chiral perturbation theory to one loop", Annals of Physics **158**, 142–210 (1984).

[12] J. Gasser, M. E. Sainio, and A. Svarc, "Nucleons with Chiral Loops", Nucl. Phys. B **307**, 779–853 (1988).

[13] S. Scherer and M. Schindler, *A primer for chiral perturbation theory*, Lecture Notes in Physics (Springer Berlin Heidelberg, 2011).

[14] S. Weinberg, "Nuclear forces from chiral Lagrangians", Phys. Lett. B **251**, 288–292 (1990).

[15] S. Weinberg, "Effective chiral Lagrangians for nucleon - pion interactions and nuclear forces", Nucl. Phys. B **363**, 3–18 (1991).

[16] S. Weinberg, "Three body interactions among nucleons and pions", Phys. Lett. B **295**, 114–121 (1992), arXiv:hep-ph/9209257.

[17] C. Ordonez and U. van Kolck, "Chiral lagrangians and nuclear forces", Phys. Lett. B **291**, 459–464 (1992).

[18] C. Ordonez, L. Ray, and U. van Kolck, "Nucleon-nucleon potential from an effective chiral Lagrangian", Phys. Rev. Lett. **72**, 1982–1985 (1994).

[19] C. Ordonez, L. Ray, and U. van Kolck, "The Two nucleon potential from chiral Lagrangians", Phys. Rev. C **53**, 2086–2105 (1996), arXiv:hep-ph/9511380.

[20] N. Kaiser, "Chiral 3 pi exchange N N potentials: Results for representation invariant classes of diagrams", Phys. Rev. C **61**, 014003 (2000), arXiv:nucl-th/9910044.

[21] N. Kaiser, "Chiral three pi exchange N N potentials: Results for diagrams proportional to g(A)**4 and g(A)**6", Phys. Rev. C **62**, 024001 (2000), arXiv:nucl-th/9912054.

[22] N. Kaiser, "Chiral 3 pi exchange N N potentials: Results for dominant next-to-leading order contributions", Phys. Rev. C **63**, 044010 (2001), arXiv:nucl-th/0101052.

[23] N. Kaiser, "Chiral 2 pi exchange N N potentials: Two loop contributions", Phys. Rev. C **64**, 057001 (2001), arXiv:nucl-th/0107064.

[24] N. Kaiser, "Chiral 2 pi exchange NN potentials: Relativistic 1 /M**2 corrections", Phys. Rev. C **65**, 017001 (2002), arXiv:nucl-th/0109071.

[25] E. Epelbaum, W. Gloeckle, and U.-G. Meissner, "Nuclear forces from chiral Lagrangians using the method of unitary transformation. 1. Formalism", Nucl. Phys. A **637**, 107–134 (1998), arXiv:nucl-th/9801064.

[26] E. Epelbaum, W. Gloeckle, and U.-G. Meissner, "Nuclear forces from chiral Lagrangians using the method of unitary transformation. 2. The two nucleon system", Nucl. Phys. A **671**, 295–331 (2000), arXiv:nucl-th/9910064.

[27] E. Epelbaum, W. Glockle, and U.-G. Meissner, "The Two-nucleon system at next-to-next-to-next-to-leading order", Nucl. Phys. A **747**, 362–424 (2005), arXiv:nucl-th/0405048.

[28] E. Epelbaum, A. Nogga, W. Gloeckle, H. Kamada, U. G. Meissner, and H. Witala, "Three nucleon forces from chiral effective field theory", Phys. Rev. C **66**, 064001 (2002), arXiv:nucl-th/0208023.

[29] D. R. Entem and R. Machleidt, "Accurate charge dependent nucleon nucleon potential at fourth order of chiral perturbation theory", Phys. Rev. C **68**, 041001 (2003), arXiv:nucl-th/0304018.

[30] A. Ekström et al., "Optimized Chiral Nucleon-Nucleon Interaction at Next-to-Next-to-Leading Order", Phys. Rev. Lett. **110**, 192502 (2013), arXiv:1303.4674 [nucl-th].

[31] B. D. Carlsson, A. Ekström, C. Forssén, D. F. Strömberg, G. R. Jansen, O. Lilja, M. Lindby, B. A. Mattsson, and K. A. Wendt, "Uncertainty analysis and order-by-order optimization of chiral nuclear interactions", Phys. Rev. X **6**, 011019 (2016), arXiv:1506.02466 [nucl-th].

[32] M. R. Schindler and D. R. Phillips, "Bayesian Methods for Parameter Estimation in Effective Field Theories", Ann. Phys. **324**, [Erratum: Ann. Phys. 324, 2051–2055 (2009)], 682–708 (2009), arXiv:0808.3643 [hep-ph].

[33] R. J. Furnstahl, D. R. Phillips, and S. Wesolowski, "A recipe for EFT uncertainty quantification in nuclear physics", J. Phys. G **42**, 034028 (2015), arXiv:1407.0657 [nucl-th].

[34] R. J. Furnstahl, N. Klco, D. R. Phillips, and S. Wesolowski, "Quantifying truncation errors in effective field theory", Phys. Rev. C **92**, 024005 (2015), arXiv:1506.01343 [nucl-th].

[35] J. A. Melendez, S. Wesolowski, and R. J. Furnstahl, "Bayesian truncation errors in chiral effective field theory: nucleon-nucleon observables", Phys. Rev. C **96**, 024003 (2017), arXiv:1704.03308 [nucl-th].

[36] J. A. Melendez, R. J. Furnstahl, D. R. Phillips, M. T. Pratola, and S. Wesolowski, "Quantifying Correlated Truncation Errors in Effective Field Theory", Phys. Rev. C **100**, 044001 (2019), arXiv:1904.10581 [nucl-th].

[37] I. Svensson, A. Ekström, and C. Forssén, "Bayesian parameter estimation in chiral effective field theory using the hamiltonian monte carlo method", Phys. Rev. C **105**, 014004 (2022).

[38] I. Svensson, A. Ekström, and C. Forssén, "Bayesian estimation of the low-energy constants up to fourth order in the nucleon-nucleon sector of chiral effective field theory", Phys. Rev. C **107**, 014001 (2023), arXiv:2206.08250 [nucl-th].

[39] S Wesolowski, R. J. Furnstahl, J. A. Melendez, and D. R. Phillips, "Exploring bayesian parameter estimation for chiral effective field theory using nucleon-nucleon phase shifts", J. Phys. G **46**, 045102 (2019).

[40] S. Wesolowski, I. Svensson, A. Ekström, C. Forssén, R. J. Furnstahl, J. A. Melendez, and D. R. Phillips, "Rigorous constraints on three-nucleon forces in chiral effective field theory from fast and accurate calculations of few-body observables", Phys. Rev. C **104**, 064001 (2021), arXiv:2104.04441 [nucl-th].

[41] D. R. Entem, N. Kaiser, R. Machleidt, and Y. Nosyk, "Dominant contributions to the nucleon-nucleon interaction at sixth order of chiral perturbation theory", Phys. Rev. C **92**, 064001 (2015), arXiv:1505.03562 [nucl-th].

[42] P. Reinert, H. Krebs, and E. Epelbaum, "Semilocal momentum-space regularized chiral two-nucleon potentials up to fifth order", Eur. Phys. J. A **54**, 86 (2018), arXiv:1711.08821 [nucl-th].

[43] B. R. Barrett, P. Navratil, and J. P. Vary, "Ab initio no core shell model", Prog. Part. Nucl. Phys. **69**, 131–181 (2013).

[44] G. Hagen, T. Papenbrock, M. Hjorth-Jensen, and D. J. Dean, "Coupled-cluster computations of atomic nuclei", Rept. Prog. Phys. **77**, 096302 (2014), arXiv:1312.7872 [nucl-th].

[45] A. Ekström, C. Forssén, G. Hagen, G. R. Jansen, W. Jiang, and T. Papenbrock, "What is ab initio in nuclear theory?", Front. Phys. **11**, 1129094 (2023), arXiv:2212.11064 [nucl-th].

[46] R. Machleidt, "What is ab initio?", Few Body Syst. **64**, 77 (2023), arXiv:2307.06416 [nucl-th].

[47] P. Navratil, J. P. Vary, and B. R. Barrett, "Properties of C-12 in the ab initio nuclear shell model", Phys. Rev. Lett. **84**, 5728–5731 (2000), arXiv:nucl-th/0004058.

[48] G. Hagen et al., "Neutron and weak-charge distributions of the ^{48}Ca nucleus", Nature Phys. **12**, 186–190 (2015), arXiv:1509.07169 [nucl-th].

[49] P. Arthuis, C. Barbieri, M. Vorabbi, and P. Finelli, "*AbInitio* Computation of Charge Densities for Sn and Xe Isotopes", Phys. Rev. Lett. **125**, 182501 (2020), arXiv:2002.02214 [nucl-th].

[50] B. Hu et al., "Ab initio predictions link the neutron skin of ^{208}Pb to nuclear forces", Nature Phys. **18**, 1196–1200 (2022), arXiv:2112.01125 [nucl-th].

[51] B. A. Brown, "Neutron radii in nuclei and the neutron equation of state", Phys. Rev. Lett. **85**, 5296–5299 (2000).

[52] R. Essick, I. Tews, P. Landry, and A. Schwenk, "Astrophysical Constraints on the Symmetry Energy and the Neutron Skin of Pb208 with Minimal Modeling Assumptions", Phys. Rev. Lett. **127**, 192701 (2021), arXiv:2102.10074 [nucl-th].

[53] J. M. Lattimer, "Neutron stars and the dense matter equation of state", Astrophys. Space Sci. **336**, 67–74 (2011).

[54] T. Dietrich, M. W. Coughlin, P. T. H. Pang, M. Bulla, J. Heinzel, L. Issa, I. Tews, and S. Antier, "Multimessenger constraints on the neutron-star equation of state and the Hubble constant", Science **370**, 1450–1453 (2020), arXiv:2002.11355 [astro-ph.HE].

[55] J. C. Hardy and I. S. Towner, "Superallowed $0^+ \to 0^+$ nuclear β decays: 2014 critical survey, with precise results for V_{ud} and CKM unitarity", Phys. Rev. C **91**, 025501 (2015), arXiv:1411.5987 [nucl-ex].

[56] L. Hayen, "Standard model $\mathcal{O}(\alpha)$ renormalization of g_A and its impact on new physics searches", Phys. Rev. D **103**, 113001 (2021), arXiv:2010.07262 [hep-ph].

[57] V. Cirigliano, W. Dekens, J. De Vries, M. L. Graesser, E. Mereghetti, S. Pastore, and U. Van Kolck, "New Leading Contribution to Neutrinoless Double-β Decay", Phys. Rev. Lett. **120**, 202001 (2018), arXiv:1802.10097 [hep-ph].

[58] V. Cirigliano et al., "Neutrinoless Double-Beta Decay: A Roadmap for Matching Theory to Experiment", (2022), arXiv:2203.12169 [hep-ph].

[59] D. B. Kaplan, M. J. Savage, and M. B. Wise, "Nucleon - nucleon scattering from effective field theory", Nucl. Phys. B **478**, 629–659 (1996), arXiv:nucl-th/9605002.

[60] A. Nogga, R. G. E. Timmermans, and U. van Kolck, "Renormalization of one-pion exchange and power counting", Phys. Rev. C **72**, 054006 (2005), arXiv:nucl-th/0506005.

[61] M. Pavon Valderrama and E. Ruiz Arriola, "Renormalization of NN interaction with chiral two pion exchange potential: Non-central phases", Phys. Rev. C **74**, [Erratum: Phys.Rev.C 75, 059905 (2007)], 064004 (2006), arXiv:nucl-th/0507075.

[62] D. B. Kaplan, M. J. Savage, and M. B. Wise, "A New expansion for nucleon-nucleon interactions", Phys. Lett. B **424**, 390–396 (1998), arXiv:nucl-th/9801034.

[63] D. B. Kaplan, M. J. Savage, and M. B. Wise, "Two nucleon systems from effective field theory", Nucl. Phys. B **534**, 329–355 (1998), arXiv:nucl-th/9802075.

[64] S. Fleming, T. Mehen, and I. W. Stewart, "NNLO corrections to nucleon-nucleon scattering and perturbative pions", Nucl. Phys. A **677**, 313–366 (2000), arXiv:nucl-th/9911001.

[65] W. Frank, D. J. Land, and R. M. Spector, "Singular potentials", Rev. Mod. Phys. **43**, 36–98 (1971).

[66] S. R. Beane, P. F. Bedaque, L. Childress, A. Kryjevski, J. McGuire, and U. van Kolck, "Singular potentials and limit cycles", Phys. Rev. A **64**, 042103 (2001).

[67] S. Wu and B. Long, "Perturbative NN scattering in chiral effective field theory", Phys. Rev. C **99**, 024003 (2019).

[68] M. C. Birse, "Power counting with one-pion exchange", Phys. Rev. C **74**, 014003 (2006), arXiv:nucl-th/0507077.

[69] B. Long and U. van Kolck, "Renormalization of Singular Potentials and Power Counting", Ann. Phys. **323**, 1304–1323 (2008), arXiv:0707.4325 [quant-ph].

[70] M. Pavon Valderrama and E. Ruiz Arriola, "Renormalization of the deuteron with one pion exchange", Phys. Rev. C **72**, 054002 (2005), arXiv:nucl-th/0504067.

[71] M. Pavon Valderrama, "Perturbative Renormalizability of Chiral Two Pion Exchange in Nucleon-Nucleon Scattering: P- and D-waves", Phys. Rev. C **84**, 064002 (2011), arXiv:1108.0872 [nucl-th].

[72] C. J. Yang, "Do we know how to count powers in pionless and pionful effective field theory?", Eur. Phys. J. A **56**, 96 (2020), arXiv:1905.12510 [nucl-th].

[73] M. Pavón Valderrama, M. Sánchez Sánchez, C. J. Yang, B. Long, J. Carbonell, and U. van Kolck, "Power Counting in Peripheral Partial Waves: The Singlet Channels", Phys. Rev. C **95**, 054001 (2017), arXiv:1611.10175 [nucl-th].

[74] M. P. Valderrama, "Perturbative renormalizability of chiral two pion exchange in nucleon-nucleon scattering", Phys. Rev. C **83**, 024003 (2011), arXiv:0912.0699 [nucl-th].

[75] B. Long and C. J. Yang, "Short-range nuclear forces in singlet channels", Phys. Rev. C **86**, 024001 (2012), arXiv:1202.4053 [nucl-th].

[76] B. Long and C.-J. Yang, "Renormalizing chiral nuclear forces: a case study of $^3P_0$", Phys. Rev. C **84**, 057001 (2011).

[77] B. Long and C.-J. Yang, "Renormalizing chiral nuclear forces: triplet channels", Phys. Rev. C **85**, 034002 (2012).

[78] C. J. Yang, "Chiral potential renormalized in harmonic-oscillator space", Phys. Rev. C **94**, 064004 (2016), arXiv:1610.01350 [nucl-th].

[79] U. van Kolck, "The Problem of Renormalization of Chiral Nuclear Forces", Front. Phys. **8**, 79 (2020), arXiv:2003.06721 [nucl-th].

[80] H. W. Griesshammer, "A Consistency Test of EFT Power Countings from Residual Cutoff Dependence", Eur. Phys. J. A **56**, 118 (2020), arXiv:2004.00411 [nucl-th].

[81] V. G. J. Stoks, R. A. M. Klomp, M. C. M. Rentmeester, and J. J. de Swart, "Partial wave analaysis of all nucleon-nucleon scattering data below 350-MeV", Phys. Rev. C **48**, 792–815 (1993).

[82] R. Peng, S. Lyu, and B. Long, "Perturbative chiral nucleon–nucleon potential for the $^3P_0$ partial wave", Commun. Theor. Phys. **72**, 095301 (2020), arXiv:2011.13186 [nucl-th].

[83] C. J. Yang, A. Ekström, C. Forssén, and G. Hagen, "Power counting in chiral effective field theory and nuclear binding", Phys. Rev. C **103**, 054304 (2021), arXiv:2011.11584 [nucl-th].

[84] D. J. Gross and F. Wilczek, "Asymptotically Free Gauge Theories - I", Phys. Rev. D **8**, 3633–3652 (1973).

[85] R. Gupta, "Introduction to lattice QCD: Course", in Les Houches Summer School in Theoretical Physics, Session 68: Probing the Standard Model of Particle Interactions (1997), pp. 83–219, arXiv:hep-lat/9807028.

[86] C. C. Chang et al., "A per-cent-level determination of the nucleon axial coupling from quantum chromodynamics", Nature **558**, 91–94 (2018), arXiv:1805.12130 [hep-lat].

[87] S. Aoki and T. Doi, "Lattice QCD and baryon-baryon interactions: HAL QCD method", Front. in Phys. **8**, 307 (2020), arXiv:2003.10730 [hep-lat].

[88] E. Fermi, "Tentativo di una teoria dell'emissione dei raggi beta", Ric. Sci. **4**, 491–495 (1933).

[89] A. Glick-Magid and D. Gazit, "A formalism to assess the accuracy of nuclear-structure weak interaction effects in precision β-decay studies", J. Phys. G **49**, 105105 (2022), arXiv:2107.10588 [nucl-th].

[90] M. E. Peskin and D. V. Schroeder, *An Introduction to quantum field theory* (Addison-Wesley, Reading, USA, 1995).

[91] R. Machleidt and D. R. Entem, "Chiral effective field theory and nuclear forces", Phys. Rep. **503**, 1–75 (2011), arXiv:1105.2919 [nucl-th].

[92] E. E. Jenkins and A. V. Manohar, "Baryon chiral perturbation theory using a heavy fermion Lagrangian", Phys. Lett. B **255**, 558–562 (1991).

[93] H. Georgi, "An Effective Field Theory for Heavy Quarks at Low-energies", Phys. Lett. B **240**, 447–450 (1990).

[94] N. Kaiser, R. Brockmann, and W. Weise, "Peripheral nucleon-nucleon phase shifts and chiral symmetry", Nucl. Phys. A **625**, 758–788 (1997), arXiv:nucl-th/9706045.

[95] N. Kaiser, S. Gerstendorfer, and W. Weise, "Peripheral NN scattering: Role of delta excitation, correlated two pion and vector meson exchange", Nucl. Phys. A **637**, 395–420 (1998), arXiv:nucl-th/9802071.

[96] K. M. Case, "Singular potentials", Phys. Rev. **80**, 797–806 (1950).

[97] A. Bastai, L. Bertocchi, S. Fubini, G. Furlan, and M. Tonin, "On the treatment of singular bethe-salpeter equations", en, Nuovo Cim **30**, 1512–1531 (1963).

[98] H.-W. Hammer and B. G. Swingle, "On the limit cycle for the 1/r2 potential in momentum space", Ann. Phys. **321**, 306–317 (2006).

[99] E. Epelbaum and J. Gegelia, "Regularization, renormalization and 'peratization' in effective field theory for two nucleons", Eur. Phys. J. A **41**, 341–354 (2009), arXiv:0906.3822 [nucl-th].

[100] E. Epelbaum, A. M. Gasparyan, J. Gegelia, and U.-G. Meißner, "How (not) to renormalize integral equations with singular potentials in effective field theory", Eur. Phys. J. A **54**, 186 (2018), arXiv:1810.02646 [nucl-th].

[101] E. Epelbaum and U. G. Meissner, "On the Renormalization of the One-Pion Exchange Potential and the Consistency of Weinberg's Power Counting", Few Body Syst. **54**, 2175–2190 (2013), arXiv:nucl-th/0609037.

[102] E. Epelbaum, H. Krebs, and U. G. Meißner, "Improved chiral nucleon-nucleon potential up to next-to-next-to-next-to-leading order", Eur. Phys. J. A **51**, 53 (2015), arXiv:1412.0142 [nucl-th].

[103] A. M. Gasparyan and E. Epelbaum, ""renormalization-group-invariant effective field theory" for few-nucleon systems is cutoff dependent", Phys. Rev. C **107**, 034001 (2023), arXiv:2210.16225 [nucl-th].

[104] M. Pavon Valderrama, "Scattering amplitudes versus potentials in nuclear effective field theory: is there a potential compromise?", (2019), arXiv:1902.08172 [nucl-th].

[105] R. N. Pérez, J. E. Amaro, and E. R. Arriola, "Coarse-grained potential analysis of neutron-proton and proton-proton scattering below the pion production threshold", Phys. Rev. C **88**, 064002 (2013).

[106] R. Navarro Pérez, J. E. Amaro, and E. Ruiz Arriola, "Partial-wave analysis of nucleon-nucleon scattering below the pion-production threshold", Phys. Rev. C **88**, 024002 (2013).

[107] W. Glöckle, *The Quantum Mechanical Few-body Problem* (Springer-Verlag, Berlin Heidelberg, 1983).

[108] J. Bystricky, F. Lehar, and P. Winternitz, "Formalism of Nucleon-Nucleon Elastic Scattering Experiments", J. Phys. (France) **39**, 1 (1978).

[109] K. Erkelenz, R. Alzetta, and K. Holinde, "Momentum space calculations and helicity formalism in nuclear physics", Nucl. Phys. A **176**, 413–432 (1971).

[110] J. J. Sakurai and J. Napolitano, *Modern quantum mechanics*, 2nd ed. (Cambridge University Press, 2017).

[111] J. R. Taylor, *Scattering Theory: The quantum Theory on Nonrelativistic Collisions* (Wiley, New York, 1972).

[112] M. I. Haftel and F. Tabakin, "Nuclear saturation and the smoothness of nucleon-nucleon potentials", Nucl. Phys. A **158**, 1–42 (1970).

[113] R. H. Landau, *Quantum mechanics ii: a second course in quantum theory*, 2nd ed (Wiley, New York, 1996).

[114] G. E. Brown, A. D. Jackson, and T. T. S. Kuo, "Nucleon-nucleon potential and minimal relativity", Nucl. Phys. A **133**, 481–492 (1969).

[115] H. P. Stapp, T. J. Ypsilantis, and N. Metropolis, "Phase shift analysis of 310-MeV proton proton scattering experiments", Phys. Rev. **105**, 302–310 (1957).

[116] M. S. Hussein and L. F. Canto, *Scattering theory of molecules, atoms and nuclei* (World Scientific Publishing Company, Singapore, SINGAPORE, 2012).

[117] D. Odell, D. R. Phillips, and U. van Kolck, "Effective Field Theory for the Bound States and Scattering of a Heavy Charged Particle and a Neutral Atom", (2023), arXiv:2307.13103 [nucl-th].

[118] J. M. Blatt and L. C. Biedenharn, "The Angular Distribution of Scattering and Reaction Cross Sections", Rev. Mod. Phys. **24**, 258–272 (1952).

[119] R. G. Newton, *Scattering theory of waves and particles* (Springer-Verlag New York, Inc., 175 Fifth Avenue New York, New York, 10010 U.S.A., 1982).

[120] M. Cacciari and N. Houdeau, "Meaningful characterisation of perturbative theoretical uncertainties", JHEP **09**, 039 (2011), arXiv:1105.5152 [hep-ph].

[121] I. Svensson, A. Ekström, and C. Forssén, "Inference of the low-energy constants in delta-full chiral effective field theory including a correlated truncation error", (2023), arXiv:2304.02004 [nucl-th].

[122] I. Vernon, M. Goldstein, and R. Bower, "Galaxy formation: a bayesian uncertainty analysis", Bayesian Anal. **5(4)**, 619–669 (2010).

[123] I. Vernon, M. Goldstein, and R. Bower, "Galaxy formation: bayesian history matching for the observable universe", Statist. Sci. **29**, 81–90 (2014).

[124] I. Vernon, J. Liu, M. Goldstein, J. Rowe, J. Topping, and K. Lindsey, "Bayesian uncertainty analysis for complex systems biology models: emulation, global parameter searches and evaluation of gene functions", BMC Syst. Biol. **12**, 1 (2018).

[125] C. J. Yang, A. Ekström, C. Forssén, G. Hagen, G. Rupak, and U. van Kolck, "The importance of few-nucleon forces in chiral effective field theory", Eur. Phys. J. A **59**, 233 (2023), arXiv:2109.13303 [nucl-th].

[126] C. Mishra, A. Ekström, G. Hagen, T. Papenbrock, and L. Platter, "Two-pion exchange as a leading-order contribution in chiral effective field theory", Phys. Rev. C **106**, 024004 (2022), arXiv:2111.15515 [nucl-th].

[127] B. Long, "Improved convergence of chiral effective field theory for 1S0 of NN scattering", Phys. Rev. C **88**, 014002 (2013), arXiv:1304.7382 [nucl-th].